TECHNICAL UNIVERSITY
OF CRETE
School of Production
Engineering and Management

Industrial
Energy
Environmental
Systems
Laboratory
IEESL

DIPLOMA THESIS

HYDRAULIC ANALYSIS AND ENERGY OPTIMIZATION OF THE WATER SUPPLY NETWORK OF THE WIDER AREA OF CHANIA THROUGH DIGITAL SIMULATION AND USE OF RENEWABLE ENERGY SOURCES

Aikaterini Faidra Lapidaki

Supervisor professor: Dr. Spiros Papaefthimiou

Chania, September 2025

Abstract

This thesis investigates the hydraulic performance and energy optimization of the water supply network of the wider area of Chania. Using specialized software tools, WaterCAD and WaterGEMS, the network is digitally simulated under various demand and operational scenarios, including daily and seasonal variations. The objective is to evaluate the system's hydraulic performance, to identify inefficiencies and potential leaks and to propose energy-saving strategies.

Energy analysis and cost optimization are performed using tools such as RETScreen and Global Solar Atlas to assess the potential of integrating renewable energy sources, particularly photovoltaic systems, to reduce electricity consumption and greenhouse emissions. The results provide insights for efficient and sustainable management of the water supply network, highlighting the combined benefits of hydraulic optimization and renewable energy integration.

Περίληψη

Η παρούσα διπλωματική εργασία μελετά την υδραυλική απόδοση και βελτιστοποίηση της ενέργειας του δικτύου ύδρευσης και άρδευσης της ευρύτερης περιοχής των Χανίων. Με την χρήση των λογισμικών WaterCAD και WaterGEMS, πραγματοποιείται ψηφιακή προσομοίωση του δικτύου για πολλαπλά σενάρια ζήτησης και λειτουργίας, περιλαμβάνοντας ημερήσιες και εποχιακές μεταβολές. Η μελέτη αξιολογεί την υδραυλική απόδοση, εντοπίζει προβλήματα λειτουργίας, πιθανές διαρροές και προτείνει λύσεις για εξοικονόμηση ενέργειας, όπως η βελτιστοποίηση της λειτουργίας αντλιών και η αναβάθμιση του δικτύου.

Πραγματοποιήθηκε ενεργειακή ανάλυση με τη χρήση των RETScreen και Global Solar Atlas, για την αξιολόγηση ενσωμάτωσης ανανεώσιμων πηγών ενέργειας, κυρίως φωτοβολταϊκών, με στόχο τη μείωση της κατανάλωσης ηλεκτρικής ενέργειας και των εκπομπών αερίων του θερμοκηπίου. Τα αποτελέσματα παρέχουν χρήσιμες πληροφορίες για την αποδοτική και βιώσιμη διαχείριση του δικτύου αναδεικνύοντας τα οφέλη από τον συνδυασμό υδραυλικής βελτιστοποίησης και ενσωμάτωσης ανανεώσιμων πηγών ενέργειας.

Contents

Chapter 1: Introduction 5

1.1 Importance of sustainable water supply networks 5

1.2 Study area - Water supply network 6

Chapter 2: Network analysis in WaterCAD and WaterGEMS 7

2.1 WaterCAD 8

2.2 WaterGEMS 9

2.3 Analysis of the studied network 11

2.3.1 48-hour simulation 15

2.3.2 Annual simulation 19

2.4 Energy analysis using RETScreen Expert 23

2.5 Energy analysis using Global Solar Atlas 28

2.6 Leak detection simulations 30

Chapter 3: Results 33

3.1 Hydraulic performance 34

3.2 Pump operation 40

3.3 Comparison of scenarios 41

3.4 Feasibility analysis of renewable integration 41

Chapter 4: Conclusions and proposed solutions 43

4.1 Summary of key findings 44

4.2 Proposed solutions and implementation strategies 46

Bibliography 47

Chapter 1: Introduction

1.1 Importance of sustainable water supply networks

Water is essential in every living system and vital in public health, agriculture, industry and ecosystem balance. With the increase of population in urban areas, the demand for efficient and cost-effective water sources also rises, along with the operational complexity.

Sustainable water supply networks are fundamental for ensuring the efficient and equitable distribution of water. They play a crucial role in reducing losses, maximizing operational expenses, and safeguarding priceless water supplies. Inefficiencies can be found, non-revenue water can be decreased, and focused actions can be planned with the use of the IWA Water Balance and performance indicators [1].

<table>
<tr><td rowspan="10">System Input Volume</td><td rowspan="3">Authorised Consumption</td><td rowspan="2">Billed Authorised Consumption</td><td>Billed Metered Consumption (including water exported)</td><td rowspan="2">Revenue Water</td></tr>
<tr><td>Billed Unmetered Consumption</td></tr>
<tr><td rowspan="2">Unbilled Authorised Consumption</td><td>Unbilled Metered Consumption</td><td rowspan="7">Non-Revenue Water (NRW)</td></tr>
<tr><td>Unbilled Unmetered Consumption</td></tr>
<tr><td rowspan="5">Water Losses</td><td rowspan="2">Apparent* Losses</td><td>Unauthorised Consumption</td></tr>
<tr><td>Metering Inaccuracies</td></tr>
<tr><td rowspan="3">Real* Losses</td><td>Leakage on Transmission and/or Distribution Mains</td></tr>
<tr><td>Leakage and Overflows at Utility's Storage Tanks</td></tr>
<tr><td>Leakage on Service Connections up to the measurement point</td></tr>
</table>

Figure 1: *IWA Water Balance framework*

The above framework's application supports long-term planning for sustainable water management. In addition to adjusting to the environmental issue, energy use concerns, and economic constraints, this is essential for tackling climatic variability, urbanization, and rising water demand. In the water supply network of Chania, using the IWA Water Balance helps pinpoint critical zones with high leakage or unmetered consumption [2], [3].

A smart water network is an advanced water supply system that uses automated controls to monitor and manage water distribution in real time. These systems enable rapid detection of leaks and inefficiencies, reducing water loss by up to 30%, while boosting energy efficiency through better control of pumping and treatment processes. By providing accurate data on consumption patterns and infrastructure status, smart water networks enable proactive

maintenance and decision-making, with results such as extended lifespan of water infrastructure and reduced operational costs. Furthermore, the ability to enhance the resilience of water supplies against droughts and contamination events ensures consistent access to clean water while minimizing environmental impact. To fulfill the increasing demand and successfully adapt to climate change, smart technology integration into water delivery networks is crucial [4], [5], [6], [7].

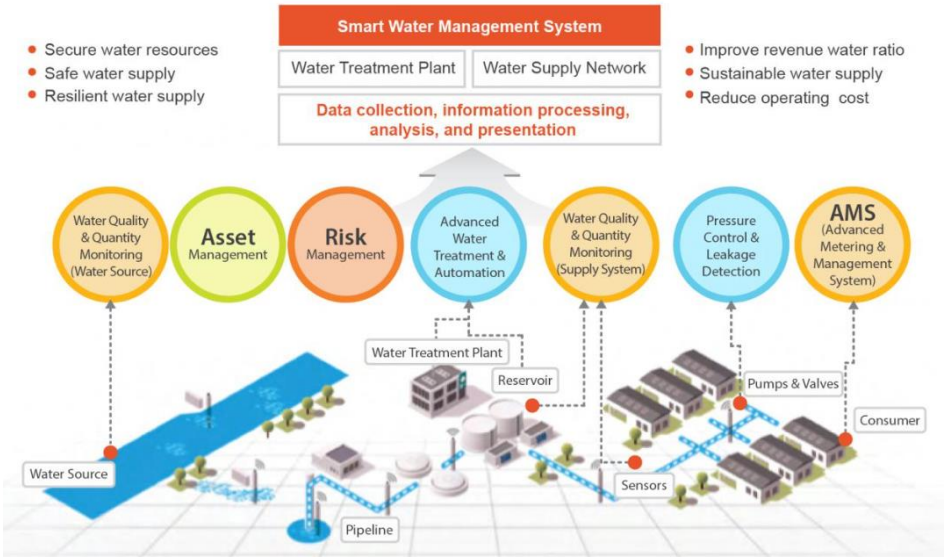

***Figure 2**: Smart water networks*

Among the various emerging technologies that support sustainable operation of water supply networks is the integration of renewable energy systems under net metering. This allows municipalities to offset energy consumed in water-related processes, such as pumping, by generating and utilizing their own green electricity, typically by solar photovoltaics.

1.2 Study area - Water supply network

The studied water distribution network is located in the broader area of Chania. It starts from the west and ends in the east, extending across multiple municipalities, including Platanias, Souda, Chania and Akrotiri Peninsula. The region is characterized by a combination of urban, suburban and rural landscapes, with significant variations in elevation ranging from sea level to over 200 meters, making hydraulic modeling particularly important for accurate analysis and system optimization [8].

The Municipality of Chania has a population of 111,375 residents, based on the population census of 2021, which accounts for roughly 17,8% of the total population of Crete. The western part of the study area can experience significant seasonal population surges during the summer months due to tourism. This seasonal variability leads to fluctuating water demands, particularly in coastal and tourist-heavy regions.

The region includes agricultural zones, especially in Platanias and Souda, where a considerable portion of the land is used for olive groves, citrus cultivation and greenhouse farming. These agricultural needs increase the demand, not only for residential use but also for irrigation purposes, especially during the dry season.

Chania has a wet and dry season, with rain concentrated from late September to late April. These months strongly affect water demand the rest of the year, especially due to the water scarcity. During the summer, reliance on stored water in reservoirs and groundwater sources increases, while in the rainy months pumping needs may decrease [9].

These seasonal fluctuations in rainfall and water availability directly influence the operation of the network.

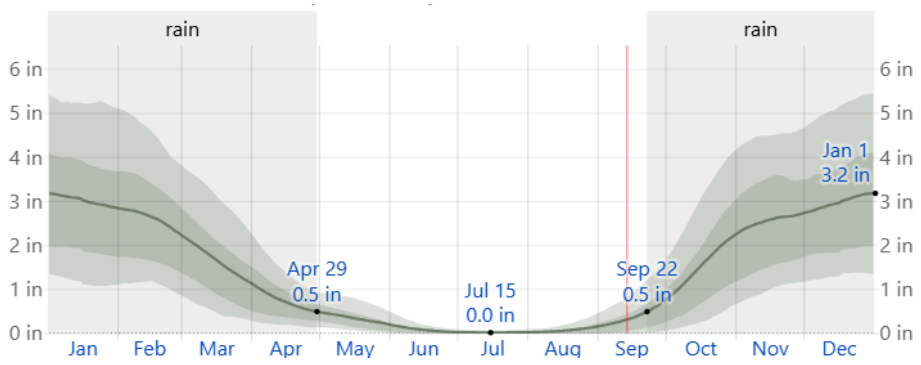

Figure 3: *Average monthly rainfall in Chania*

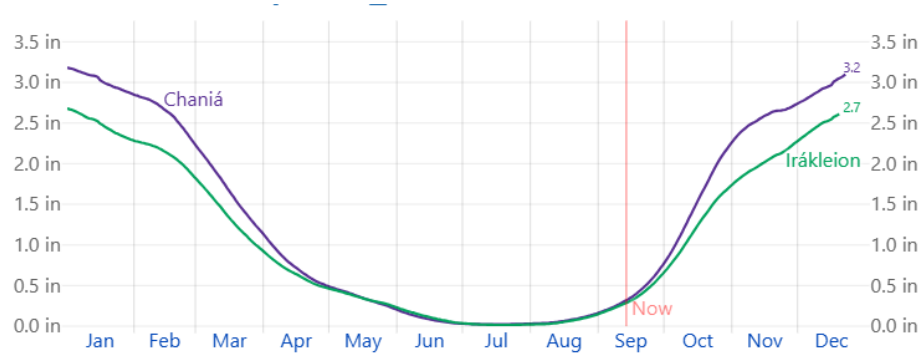

Figure 4: *Average monthly rainfall in Chania and Heraklion*

Chapter 2: Network analysis in WaterCAD and WaterGEMS

2.1 WaterCAD

WaterCAD is a software program developed by Bentley, used for hydraulic modeling and water quality analysis in water distribution systems. It supports a wide range of features, including steady-state and extended-period simulations (EPS) with key network components, such as pumps, tanks and valves.

Additional features include detailed hydraulic network analysis, scenario management and comparison and automated fire flow assessments. The software also facilitates pipe flushing studies, pressure zone analysis and energy cost evaluation. Moreover, it integrates Darwin Calibrator and Darwin Scheduler, enabling the manual adjustment of parameters to enhance model accuracy.

In this thesis, the academic version of Bentley OpenFlows WaterCAD 2024 is employed, providing full access to WaterCAD's core features.

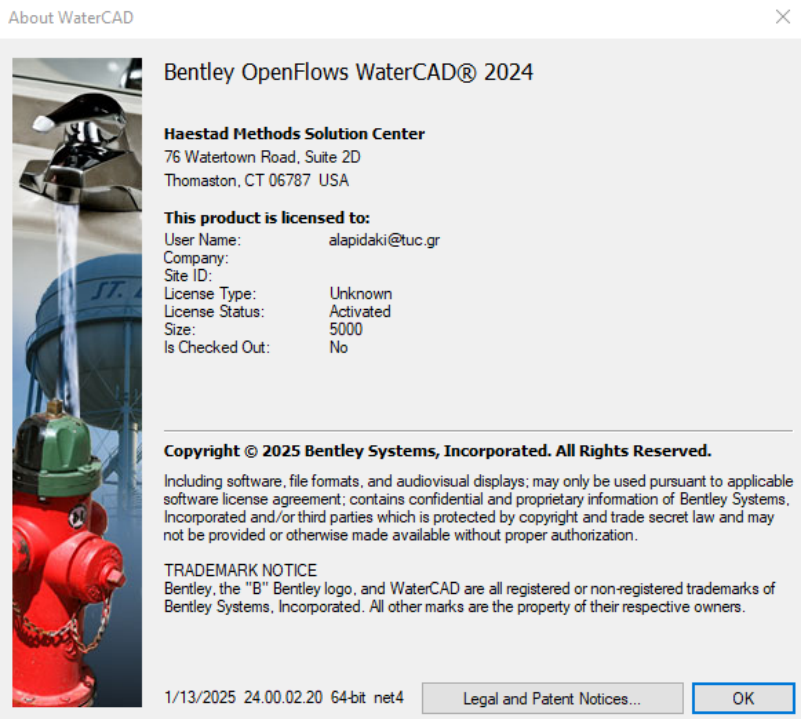

Figure 5: *WaterCAD's information*

2.2 WaterGEMS

WaterGEMS, also developed by Bentley, is an advanced hydraulic modeling software used for the design, analysis, and optimization of water distribution systems. It includes all the features of WaterCAD, along with enhanced functionalities for modeling more complex systems and operational scenarios. Its seamless integration with GIS platforms significantly enhances its modeling power, allowing users to build, edit, and map water distribution models within the GIS environment while displaying simulation results as GIS-based thematic maps.

Among its extended capabilities, WaterGEMS incorporates the Pipe Renewal Planner, a tool designed to rank pipe segments based on performance metrics, including break history, criticality, capacity and hydraulic risk. Additional attributes, such as pipe material, pipe width, construction year and location, can also be considered to identify high-risk pipes for maintenance planning.

Another feature is Darwin Calibrator, which adjusts various parameters, such as pipe roughness, demands, flow rates and aligning the model with realistic network behavior. Then, it can identify potential leakage by detecting inconsistencies between simulated and observed data. Darwin Scheduler, on the other hand, performs optimization of pump operation by determining the most efficient strategies for both fixed- and variable-speed pumps aiming to reduce energy consumption and overall operating costs.

The software also contains Darwin Designer, which performs automated or manual design processes based on input hydraulic constraints, pipe sizes and cost units. The automated design feature employs a genetic algorithm to evaluate various design and repair strategies based on cost minimization or benefit maximization, as opposed to WaterCAD (offers only a manual design option).

For model simplification, WaterGEMS includes Skelebrator. This tool reduces network complexity while preserving hydraulic equivalence and connectivity, relocating demands, and removing minor network elements.

Additionally, SCADAConnect provides the ability to integrate real-time SCADA data into the model simulation. This enables the assignment of actual system conditions based on flow rates and pressure data, thereby enhancing the model's calibration.

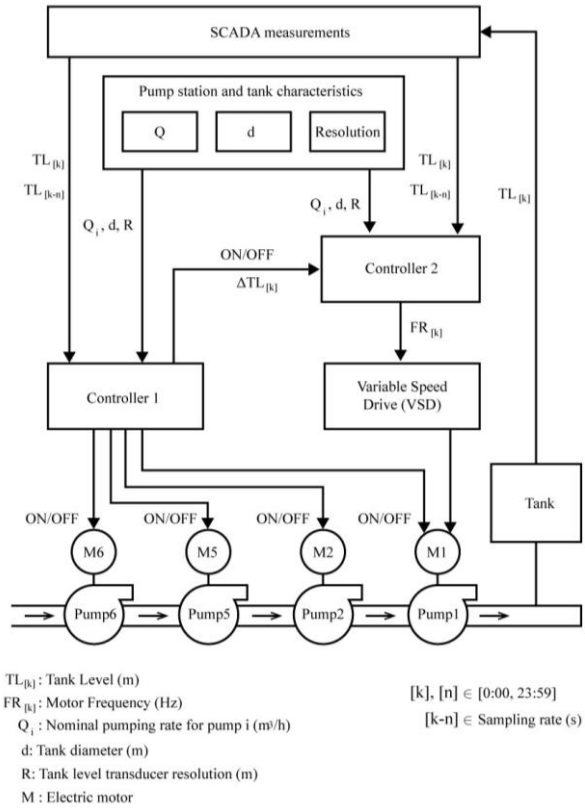

Figure 6: *SCADAConnect overview*

In this thesis, the academic version of Bentley OpenFlows WaterGEMS 2024 is employed, providing full access to all of WaterGEMS' features.

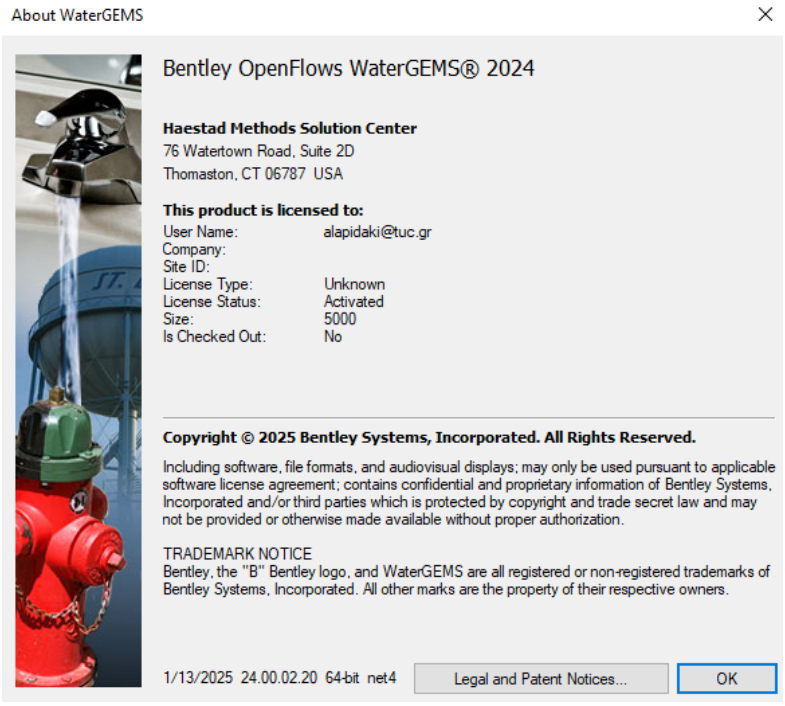

Figure 7: *WaterGEMS' information*

2.3 Analysis of the studied network

The network managed by OAK AE, is designed to supply both potable and irrigational water. The main supply of water is the Meskla springs, which are located at altitudes from 197 to 212 m. The flow from these springs is regulated by the Valsamiotis Dam, which collects and stores the water downstream of the springs and operates under a controlled release pattern to meet system demand. A steel pipeline, ranging in diameter from Φ700 to Φ1000 and extending 3,520 meters, connects the Valsamiotis tank to the main Meskla–Agia Triada–Myloniana pipeline. This pipeline functions both as a connector for transferring stored water to the Myloniana tanks and as the upstream segment of what is later referred to as the main pipeline supplying the broader Chania network [10], [11].

The dam, located near the village of Vatolakkos and named after the Valsamiotis stream, was constructed between 2005 and 2014 with co-financing from European support programs [12], [13], [14]. It is one of the largest and tallest dams of its kind in Greece, enabling the strategic regulation of flow from the Digenis stream, which drains the eastern side of Mount Asfendiles. Notably, the Meskla pipeline is closed during the dry period from April to October, with the dam ensuring the continuity of supply during these months. However, the dam is not fully waterproofed, resulting in some water loss during winter. Also, the infrastructure cost for a hydropower plant at this location would be prohibitively high for OAK AE [15], [16].

Length	335 m
Height from the ground	67,20 m
Volume	600.000 m^3
Exploitable volume	5.900.000 m^3

Figure 8: *Valsamiotis dam and its technical characteristics*

Water is conveyed by natural flow to the two tanks in Myloniana, each with a capacity of 6,500 m^3 (at an elevation of 135 m). Furthermore, in Myloniana there are 5 reservoirs, which supplement the water from the springs. The main pipeline starts with the Myloniana tank and

supplies the tanks of Perivolia (108 m, 4,000 m^3), Mournies (103 m, 6,500 m^3), Nerokourou (96 m, 6,500 m^3) and Tsikalaria (89 m, 4,000 m^3) to meet the needs of each area. There are also 3 even smaller reservoirs in Kampos that are directly connected to the network and supply the areas of Mournies and Nerokourou during the summer season.

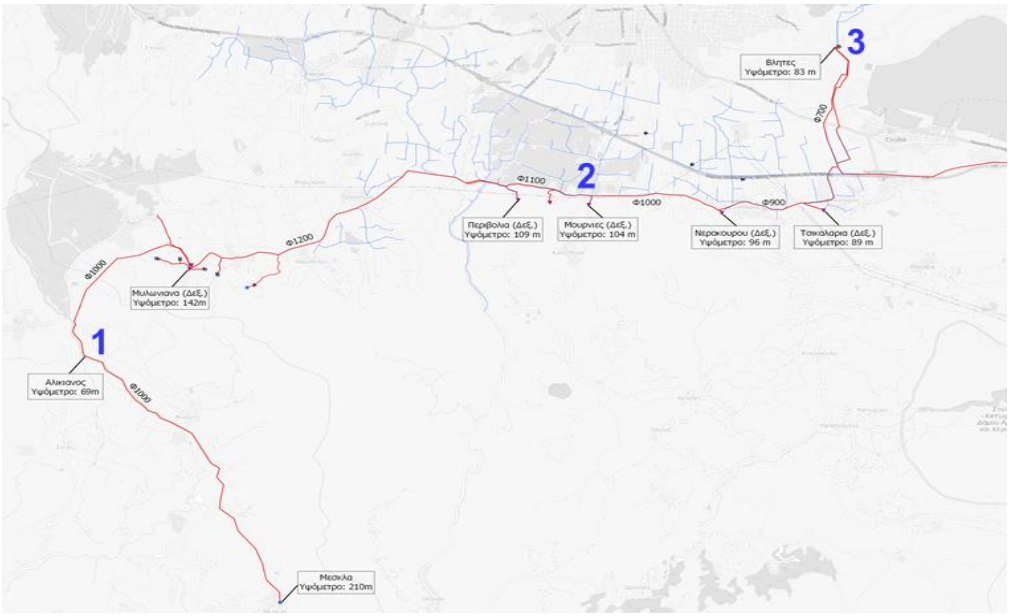

Figure 9: *Main pipeline*

The main pipeline ends at Vlites' boosting pump, where the water is concentrated in a pressure reduction tank. The water is then pumped into the Korakies tanks (215 m, 2.000 m^3 and 6.500 m^3) to meet the needs of Akrotiri. A second pipeline is used to transport water with the help of pumps from M. Chorafia to Vlites and then to the irrigation tank of Korakies. In addition, at Akrotiri there are 4 small pumps in Sternes, Mouzoura, Gouverneto to increase water pressure towards the tanks and the junctions of the area.

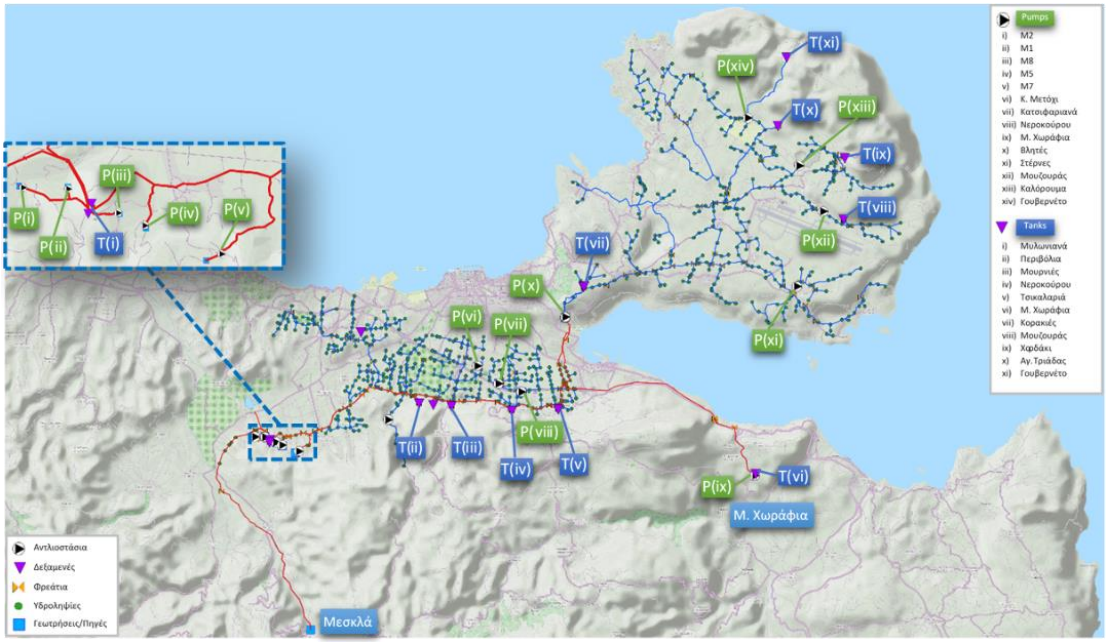

Figure 10: *Map of the network*

The critical pumps of the network:

- Myloniana pumps: In Myloniana, there are 5 reservoirs (M1, M2, M5, M7, and M8), each served by a pump that supplies water to the wider area of Chania and Akrotiri. These pumps are Pomona-type pumps. The water from M2 and M8 is directed to a pressure reduction tank at an elevation of 130 m before being routed to the Myloniana tanks. M1, M5 and M7 are connected directly to the main pipeline.

Table 1: *Technical characteristics of Myloniana pumps*

PUMP	**FLOW (m^3/h)**
M1-M2-M8	1.000
M5	300
M7	200

- Kampos pumps: There are 3 smaller reservoirs in Nerokourou, Katsifariana and Kokkino Metochi, which operate during the summer season to meet the increased demand.

- Vlites pumps: This station includes 9 pumps and supports the water supply and irrigation needs.

  Water supply: From the Myloniana tanks, water is directed to Vlites pumps by natural flow and there it is collected in a pressure reduction tank. Then, the water is pumped to the Korakies tanks to fulfill the water supply and irrigation needs of Akrotiri. On the pipeline that ends at the Korakies tanks, 6 pumps are installed, of which 2 or 3 are usually activated depending on demand conditions.

  Irrigation: From Megala Chorafia, through the 3 pumping units, the water is conveyed to the Vlites pumping stations. On this pipeline, 3 submersible booster pumps are installed, which channel the water to the Korakies irrigation tank, then distribute it to the network.

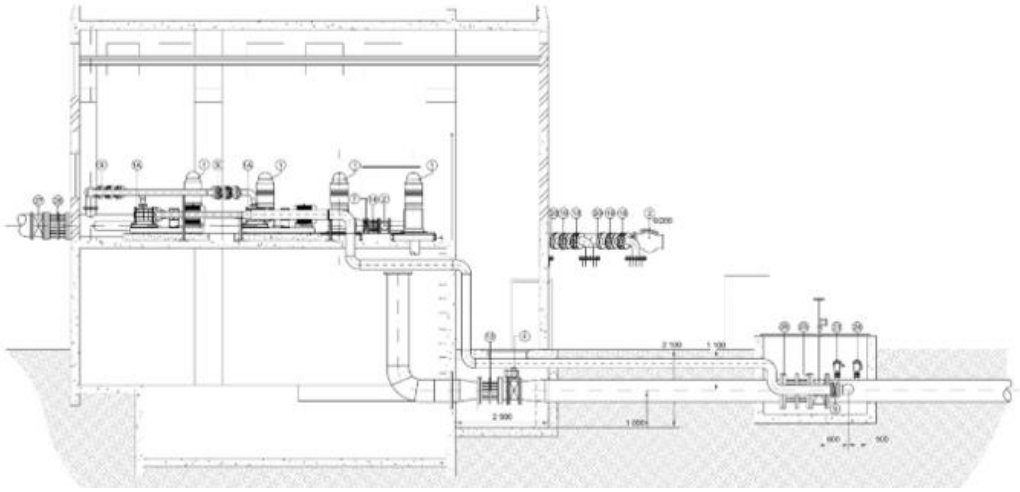

Figure 11: *Vlies pumping stations*

- Megala Chorafia pumps: The pumping stations include a circular open reinforced concrete tank (with a usable capacity of 6,400 m^3) and 9 pumps, of which 6 are used to pump water towards Vlites' pumps. The other 2 pumps are put into operation during peak hours and periods to meet demand, while the 3rd is kept as a spare.

- Akrotiri pumps: In the Akrotiri area, there are 4 small booster pumping stations to convey water to the tanks. Of these 4, the pumping station in Kaloruma is decommissioned, while the pumping station in Gouverneto is used only to meet the needs of the monastery located in the area.

Table 2: *Technical characteristics of pumps by OAK AE*

Pumps	Amount	Installed power (kW)	Flow (m^3/h)
Vlites	9	4×250, 2×186, 1×194, 2×93	4×350, 2×300, 1×300, 2×180
Megala Chorafia	9	3×75, 3×55, 2×132, 1×112	3×250, 3×250, 2×135, 1×150
Myloniana	5	3×448	3×1000, 1×300, 1×100
Katsifariana	1	-	150
Nerokourou	1	-	100
Tzivaras	6	6×200	6×250
Mouzela	2	2×90	2×150
Sternes	3	3×32	3×120
Mouzouras	3	3×15	3×40

2.3.1 48-hour simulation

The water supply network of the wider area of Chania was created in the software EPANET and was studied in WaterGEMS and WaterCAD [17], [18]. Both software concluded with the same results, with WaterGEMS operating a little faster. The network relies on gravity, which means the flow of the water is achieved mostly due to the elevation difference between the supply points and the consumption points. The network presented in Figure 12, consists of 14 tanks, 10 reservoirs and 1111 junctions.

Before modeling the network on an annual scale, a 48-hour simulation is conducted to establish a baseline understanding of its hydraulic behavior and fix any errors. This simulation serves multiple purposes, such as evaluating the network's transfer from EPANET to WaterGEMS, testing the initial control rules, verifying the pump and valve coordination and mostly creating a testing ground for the annual network.

The initial modeling stage consisted of a 24-hour simulation. This duration proved insufficient, as several tanks reached critically low levels before the simulation ended. Additionally, it was unclear whether the rules were functioning correctly, so it was extended to 48 hours. The hydraulic time step was set to 0.017 hours (≈1 minute), which ensured a smooth and detailed operation while capturing rapid changes in flow and demand.

Figure 12: *Water supply network of the wider area of Chania*

The demand centers that were transferred by the EPANET model consisted of real data obtained by OAK AE. Two patterns were used, daily and daily 1, to describe hourly consumption for every junction. The demand at each node is calculated as the product of the base demand and the pattern multiplier (Base Demand*Multiplier). When higher base demands are assigned to the nodes, smaller multipliers are required to avoid unrealistically high consumption values, while lower base demands necessitate larger multipliers to reach the same order of magnitude. Also, tank levels and pump characteristics and curves were initialized with data from OAK AE to ensure realistic results and that the simulation begins from normal flow conditions.

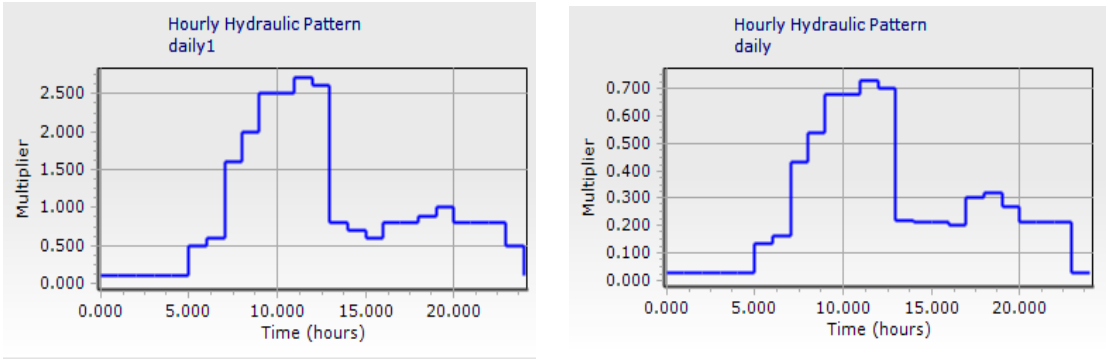

Graph 1: *Hourly patters*

At the same time, the model's architecture was reconstructed. Both PRV (pressure reducing valve) and TCV (throttle control valve) were removed since they either created inconsistencies (e.g. unrealistic pressure drops) or did not substantially contribute to the hydraulic analysis. All pipes were examined to set one-way flow restrictions on the critical ones in areas with a large elevation difference to prevent backward flow. The initial state of the pumps and pipes was reevaluated and corrected, ensuring the simulation starts with normal flow conditions without artificial constraints that could cause errors.

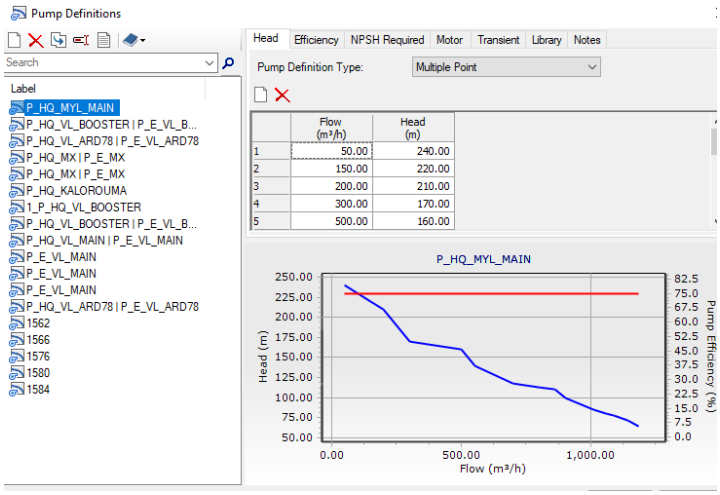

Figure 13: *Pump characteristics and curves*

The most important part of this modeling was to review all rules and set some new ones for any component not working properly, since WaterGEMS and WaterCAD are more complex than EPANET. These new rules oversee the activation of the pumps, the opening or closing of the pipes, the flow direction. This testing was crucial for confirming that the logic of the rules functioned as intended and could later be adapted for long-term simulation [19], [20].

The control rules can be grouped into three main categories:

(i) Demand-based rules, which activate pumps and open supplementary pipes when system demand exceeds predefined thresholds;

(ii) Tank-level dependent rules, designed to prevent tanks from overflowing or running dry by controlling pumps and pipe statuses according to the measured water levels;

(iii) Time-based rules, which manage the operation of the main supply lines according to the daily demand. These rules were developed to replicate the exact operational strategies of the actual network. Validation was performed by comparing simulated tank levels, flows and

pump operations, ensuring that the network maintains continuous supply throughout the whole simulation time.

The simulation control rules used to achieve this modeling are stated below.

(i) Demand-based rules

- When the system demand is greater than 1200 m^3/h and pipe MESKLA_MAIN_1 is closed, then pumps PUMP_VLITES_ARD_1, PUMP_VLITES_ARD_2, PUMP_MX_1, PUMP_MX_2, PUMP_NE, PUMP_KM and PUMP_KATS are switched on and pipe 45 is open.
- When the system demand is less than 1200 m^3/h, then pumps PUMP_VLITES_ARD_1, PUMP_VLITES_ARD_2, PUMP_MX_1, PUMP_MX_2, PUMP_NE, PUMP_KM and PUMP_KATS are switched off and pipe 45 is closed.

(ii) Tank-level dependent rules

- When Tank Myloniana level is below 1.5 m and pipe MESKLA_MAIN_1 is open, then pipe 11 is closed and pipe PI_MAIN_21 is opened.
- When Tank Myloniana level is below 1.5 m and pipe MESKLA_MAIN_1 is closed, then pumps PUMP_M1, PUMP_M2, PUMP_M5, PUMP_M7, PUMP_M8 are switched on and pipe PI_MAIN_21 is opened.
- When Tank Myloniana level is above 5.7 m, then pumps PUMP_M1, PUMP_M2, PUMP_M5, PUMP_M7, PUMP_M8 are switched off, pipe PI_MAIN_21 is closed and pipe 11 is opened.
- When Tank Freatiohremias level is above 5.9 m, then pipe VLITES_CV is closed.
- When Tank Freatiohremias level is below 1.1 m, then pipe VLITES_CV is opened.
- When Tank 3D1 level is below 2.5 m, then pumps PUMP_VLITES_YDR_1 and PUMP_VLITES_YDR_2 are switched on.
- When Tank 3D1 level is below 2,0m and pump PUMP_VLITES_YDR_1 is on, then pump PUMP_VLITES_YDR_3 is switched on.
- When Tank 3D1 level is above 6.5 m, then pumps PUMP_VLITES_YDR_1, PUMP_VLITES_YDR_2, and PUMP_VLITES_YDR_3 are switched off.
- When Tank Deyax level is below 1.0 m, then pipe PI_MAIN_DEYAX is opened.
- When Tank Deyax level is above 5.7 m, then pipe PI_MAIN_DEYAX is closed.
- When Tank Perivolia level is above 3.8 m, then pipe PI_MAIN_69 is closed.

- When Tank Perivolia level is below 1.0 m, then pipe PI_MAIN_69 is opened.
- When Tank Mournies level is above 3.6 m, then pipe 23 is closed.
- When Tank Mournies level is below 1.0 m, then pipe 23 is opened.
- When Tank Nerokourou level is above 5.3 m, then pipe 30 is closed.
- When Tank Nerokourou level is below 1.0 m, then pipe 30 is opened.
- When Tank Tsikalaria level is above 4.95 m, then pipe 14 is closed.
- When Tank Tsikalaria level is below 1.5 m, then pipe 14 is opened.
- When Tank Daratso level is above 3.8 m, then pipe PI_NK_88_126 is closed.
- When Tank Daratso level is below 1.5 m, then pipe PI_NK_88_126 is opened.
- When Tank Xordaki level is above 3.5 m, then pump PUMP_KALOROUMA is switched off.
- When Tank Xordaki level is below 1.0 m, then pump PUMP_KALOROUMA is switched on.
- When Tank MX level is above 6.0 m, then pipe 5 is closed.
- When Tank MX level is below 1.0 m, then pipe 5 is opened.
- When Tank AT level is above 5.7 m, then pipe PI_AN_VIN_T_AT is closed.
- When Tank AT level is below 1.0 m, then pipe PI_AN_VIN_T_AT is opened.

(iii) Time-based rules

- When the clock time is after 18:00, then pipe MESKLA_MAIN_1 and pipe PI_AK_84_85 are closed.
- When the clock time is before or equal to 18:00, then pipe MESKLA_MAIN_1 and pipe PI_AK_84_85 are opened.

With the 48-hour simulation completed and the control logic validated, the results will be examined in the following chapters and the model is ready to be expanded for annual analysis.

2.3.2 Annual simulation

With the 48-hour simulation completed, which validated control logic and initial conditions, the model will be expanded to an annual simulation. The annual simulation is conducted to examine and evaluate the performance over a full year, considering seasonal variations, population fluctuations due to tourism and agricultural water demands. In addition, this

simulation provides insights into the network's ability to maintain a continuous supply, ensuring that both potable and irrigation needs are met efficiently.

By examining the entire year, it is possible to model the network behavior under the conditions described. Moreover, this simulation supports the optimization of the pump's schedule and assessment of critical nodes and junctions.

Initially, the duration was converted from 48 hours to 8760 hours (1 year). The hydraulic time step was also adjusted to a 6-hour to achieve smoother results, as using a shorter time step over such a long duration would have significantly increased calculation time and risked numerical instability. This time step was chosen as a balanced compromise between efficiency and the ability to record critical changes in system operation.

To support the modeling, the consumption patterns were altered to incorporate monthly availability with data collected from OAK AE. More specifically, the patterns were modified accordingly to be annual and account for the dry period but also to be consistent with the 6-hour time step (the time step must be a multiplier of the hydraulic time step).

Daily

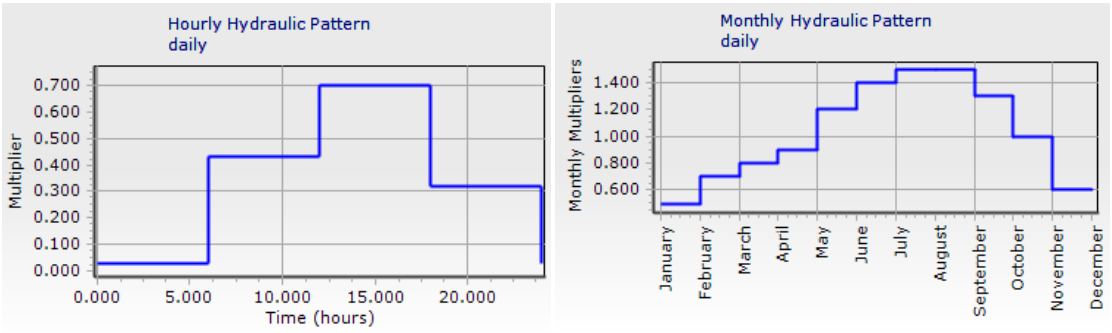

Graph 2: *Hourly & monthly patterns (Daily)*

Daily 1

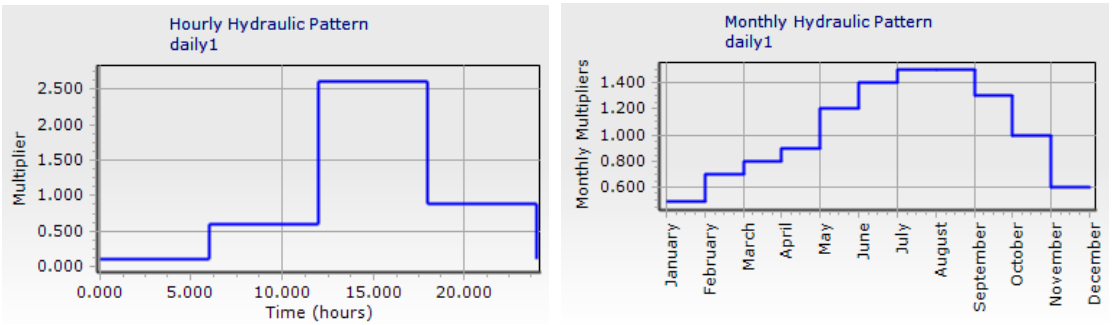

Graph 3: *Hourly & monthly patterns (Daily 1)*

As in the 48-hour simulation, the model's architecture was reviewed, PRV and TCV were removed and critical pipes and pumps were initialized to ensure normal flow conditions.

Emphasis was placed on the design of the new seasonal rule, while the previously tested control rules were retained unchanged. Due to limitations of the student edition of the software, it is not possible to use calendar variables, such as "System Month", resulting in seasonal changes being portrayed using the "Time From Start" variable, where time limits were expressed in hours from the start of the simulation.

For the annual model to work for a standard year (8760 hours=365 days), a seasonal rule had to be implemented to deliberately close the MESKLA_MAIN_1 pipe during the summer. The pipe closes for time greater or equal to 2160 hours, which equals to hours counted from the beginning of the year until the 28th of February, and less than 7296 hours, which equals to hours counted from the beginning of the year until October 31st. At that time, demand increases and it must be met by activating an array of pumping stations and alternative transmission mains. This operational shift ensures that the downstream reservoirs are maintained at acceptable levels but also results in higher energy consumption due to the increased reliance on pumping.

The MESKLA_MAIN_1 pipeline contributes most of the critical inflows of Chania's water supply network, as it transports water derived primarily from natural springs and surface sources in the Meskla area. This supply is strongly dependent on seasonal conditions: during the rainy season of autumn and winter, the upstream sources provide enough to feed the entire network by gravity, supporting both the filling of storage tanks and the reduction of pumping requirements. However, during the dry months of summer, the available water in Meskla decreases dramatically, to the point that the pipeline cannot operate as a reliable supplier.

The seasonal rule is also time-based and stated below.

- When the time from start is greater or equal to 2160 hours and less than 7296 hours, then pipe MESKLA_MAIN_1 is closed.
- When the time from start is less than 2160 hours or greater than 7296 hours, then pipe MESKLA_MAIN_1 is open.

This rule is assigned with priority level 5 to ensure that it is evaluated before the other control rules which have no priority set (when multiple rules are active simultaneously, the priority determines which rule is evaluated first). This guarantees that seasonal operational

constraints take precedence over other controls, maintaining realistic hydraulic behavior during dry and wet seasons.

During the testing of the seasonal rule, it was observed that while the command was being executed, the flow in the pipeline had already reached zero at some points due to the network-wide pressure distribution and the lack of active demand at those points in time. This observation highlights the importance of simultaneously evaluating both the controls and the flow results.

Table 3: *Tanks' characteristics*

Tank ID	Elevation Base (m)	Diameter (m)	Level Minimum (m)	Level Initial (m)	Level Maximum (m)
TANK_BALS	170.00	600.00	0.50	2.00	20.00
TANK_XORDAKI	257.00	9.70	0.50	3.00	4.00
TANK_AT	144.00	29.00	0.50	1.00	6.00
TANK_MOUZOURAS	175.00	9.00	0.50	4.00	9.00
TANK_3D1	212.00	52.00	0.50	3.50	7.00
TANK_DEYAX	108.35	37.00	0.50	6.00	6.00
TANK_DARATSO	74.00	10.00	0.50	3.00	4.00
TANK_MX	112.00	37.00	0.50	6.05	6.05
TANK_TSIKALARIA	89.00	32.00	0.50	4.00	5.00
TANK_NEROKOUROU	96.30	39.00	0.50	4.50	5.45
TANK_MOYRNIES	103.58	37.00	0.50	3.50	3.95
TANK_PERIVOLIA	108.50	36.00	0.50	3.50	3.95
TANK_MYLONIANA	136.00	53.00	0.50	3.00	6.00
FREATIOHREMIASVL	80.00	20.00	1.00	3.00	6.00

To better illustrate the flow fluctuations in the pipes during the simulation, a color-coding scale was created.

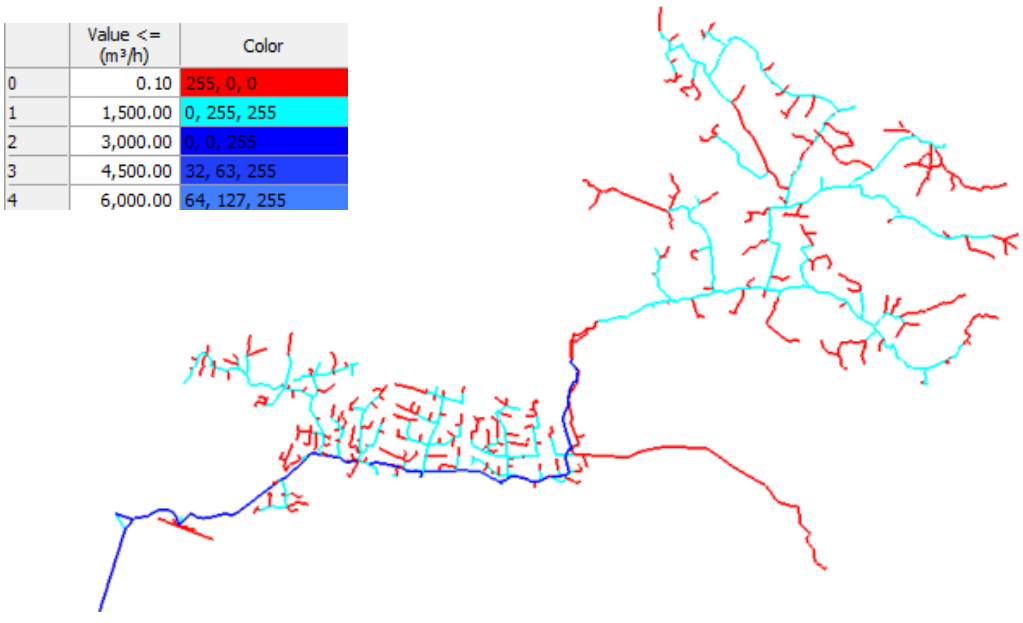

Figure 14: *Pipe flow illustrated in the network at 00.00 h*

With the annual model now fully established, seasonal variations and demand patterns have now been incorporated and the results of the simulation will be analyzed in the following chapters.

2.4 Energy analysis using RETScreen Expert

RETScreen Expert is a clean energy analysis software developed by Natural Resources Canada (NRCan). It is a tool used worldwide to evaluate energy performance, cost and environmental impact. RETScreen is widely used for analyzing energy consumption and greenhouse gas (GHG) emissions. Some of the features of the software include versatility, analysis on many green aspects and plenty of databases about climate and hydrology.

RETScreen conducts a monthly calculation on energy production for photovoltaic (PV) systems. The analysis relies on key models and data sources, such as ground-based or satellite-derived meteorological data (NASA), to evaluate the output of a PV project.

In this study, this software was employed to measure the electricity required for the pumping stations of the network, to evaluate their operational costs and emissions and to suggest a more environmentally friendly solution. All necessary data were taken into account: technical data, operational data, economic factors, performance indicators [21], [22].

The Myloniana pumping stations, which consists of five Pomona pumps (M1, M2, M5, M7, M8), was selected for this energy analysis. These pumps are very essential because it supplies many reservoirs and junctions, particularly during high demand periods. Its energy consumption is therefore a significant factor in the overall efficiency of the network.

Figure 15: *Myloniana's pumping stations*

From the annual simulation and the general operating information of the network, pump profiles were obtained for all five pumps. The annual operating hours were measured at 540 hours for each pump. Based on the fact that M1, M2, M8 have a flow of 1000 m^3/h, M5 of 300 m^3/h and M7 of 200 m^3/h, the next step was to calculate the annual consumption of electricity in kWh.

The hydraulic power of each pump was estimated using the following equation:

$$P_h = \frac{\rho \cdot g \cdot Q \cdot H}{1000}$$

Where:

- P_h = hydraulic power (kW)
- ρ = density of water (1000 kg/m^3)
- g = acceleration due to gravity (9.81 m/s^2)
- Q = flow rate of pump (m^3/s)
- H = pump head (m)
- Division by 1000 to convert watts (W) to kilowatts (kW)

The required head of the pumps was calculated as the sum of the static head and losses: $H = H_{static} + H_{losses}$

H_{static} represents the vertical elevation difference, which is 130 m in this case according to the network's information, H_{losses} corresponds to head losses due to pipe friction, bends and other minor losses.

For pumps M1, M2, M8: $P_h = \frac{1000 \cdot 9.81 \cdot 0.2778 \cdot 130}{1000} = 354.278$ kW

For pump M5: $P_h = \frac{1000 \cdot 9.81 \cdot 0.083 \cdot 150}{1000} = 122.135$ kW

For pump M7: $P_h = \frac{1000 \cdot 9.81 \cdot 0.055 \cdot 150}{1000} = 80.932$ kW

The hydraulic power was then corrected to pump efficiency to calculate the required shaft power, which represents the real power of the motor (assuming pump efficiency η = 80%).

$$P_{shaft} = \frac{P_h}{\eta}$$

For pumps M1, M2, M8: $P_{shaft} = \frac{354.278}{0.8} = 442.848$ kW

For pump M5: $P_{shaft} = \frac{122.135}{0.8} = 152.668$ kW

For pump M7: $P_{shaft} = \frac{80.932}{0.8} = 101.166$ kW

Each shaft power value was multiplied with the 540 operating hours measured and then added all together to calculate the total annual consumption of electricity. The total for all five pumps was 854483.864 kWh/year, which equals 2341.052 kWh/day.

The energy analysis conducted through RETScreen expert involves a photovoltaic solar farm, near the selected pumping station in Myloniana. The site was chosen for its large free hillside space near the pumps, where a large-scale photovoltaic plant could easily be constructed.

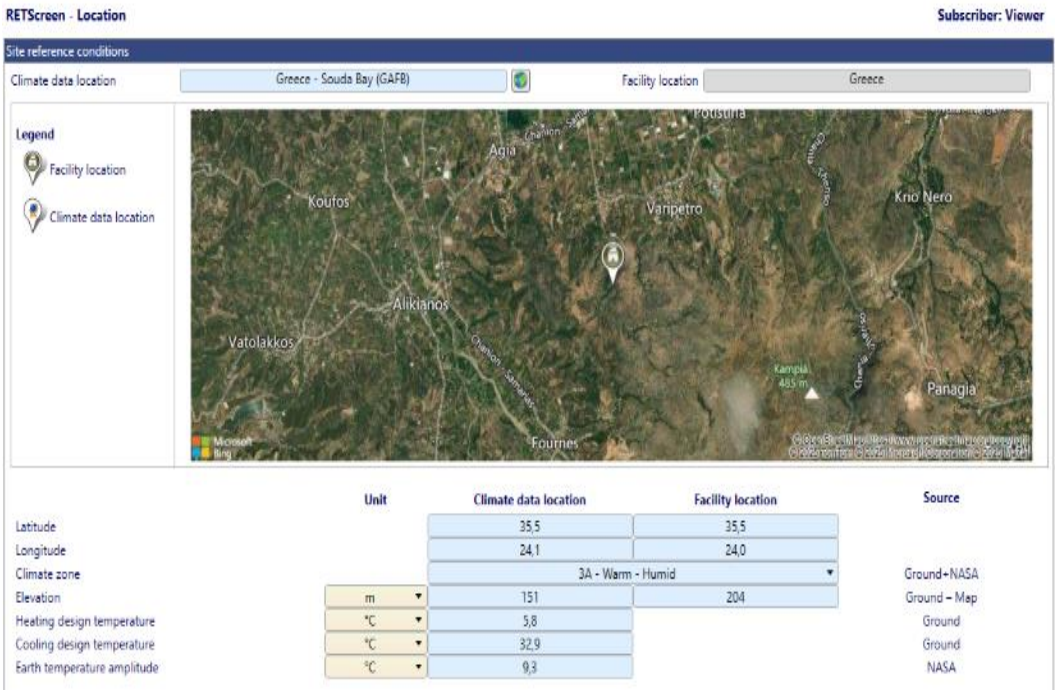

Figure 16: *Facility's location*

For the climate data location of the analysis Souda Bay (GAFB) was chosen, since it is the closest location available in the software. A photovoltaic power plant of 399 kWp is proposed for cost reduction purposes for both installation and operational costs. Moreover, the photovoltaic panels would be fixed with a tilt of 35° and azimuth of 0°, as these are the most optimal for electricity output on the suggested site. The area of panel surface is calculated to be 1860 m^2 for a quantity of 600 panels, each a size of 3.1 m^2. Therefore, a site area of 2200-

2400 m^2 is sufficient, considering ample spacing for avoiding overshadowing and enabling ease of maintenance.

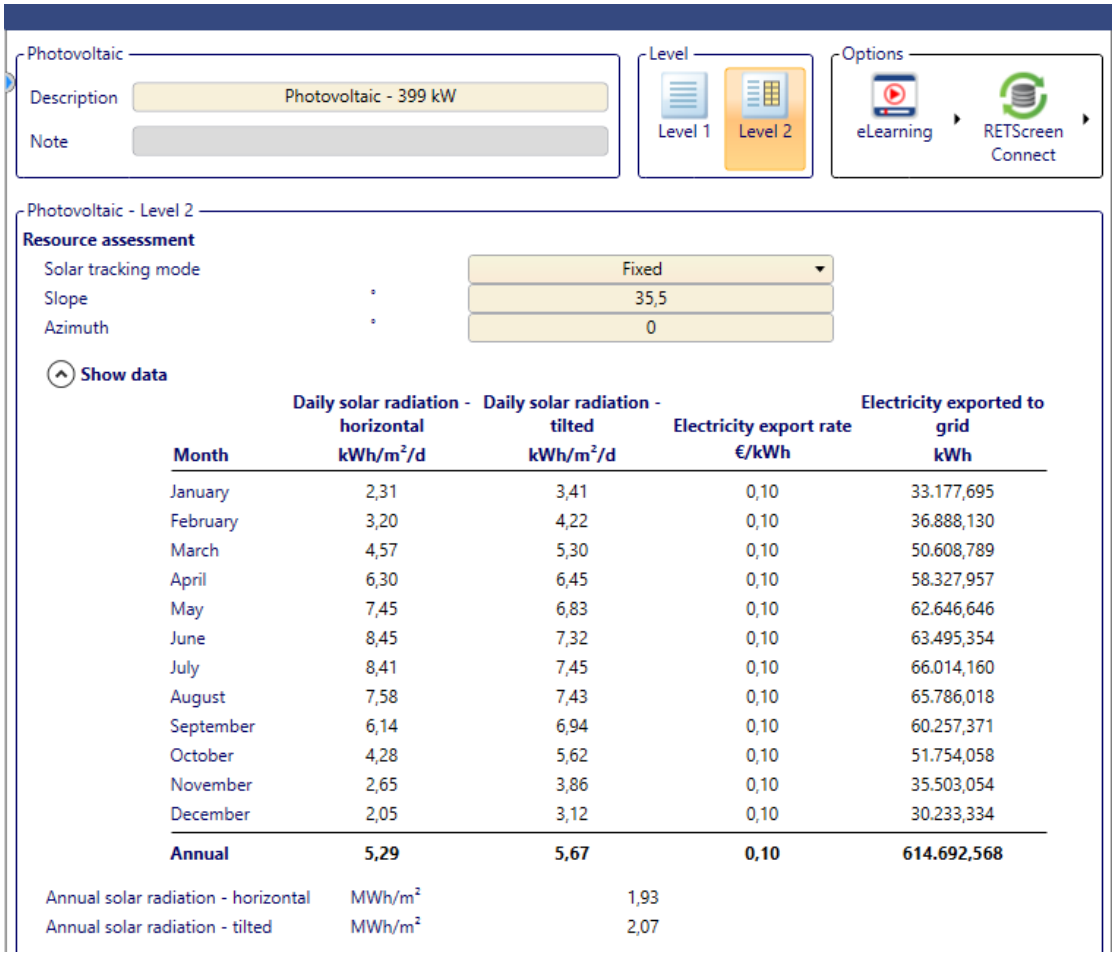

Month	Daily solar radiation - horizontal kWh/m²/d	Daily solar radiation - tilted kWh/m²/d	Electricity export rate €/kWh	Electricity exported to grid kWh
January	2,31	3,41	0,10	33.177,695
February	3,20	4,22	0,10	36.888,130
March	4,57	5,30	0,10	50.608,789
April	6,30	6,45	0,10	58.327,957
May	7,45	6,83	0,10	62.646,646
June	8,45	7,32	0,10	63.495,354
July	8,41	7,45	0,10	66.014,160
August	7,58	7,43	0,10	65.786,018
September	6,14	6,94	0,10	60.257,371
October	4,28	5,62	0,10	51.754,058
November	2,65	3,86	0,10	35.503,054
December	2,05	3,12	0,10	30.233,334
Annual	**5,29**	**5,67**	**0,10**	**614.692,568**

Figure 17: *Solar radiation data*

The manufacturer company chosen for purchasing the photovoltaic panels is Trina Solar Co, a China-based market pillar that is known for their quality and innovation in photovoltaic technologies. The proposed panel is a mono-Si TSM-DEG21C.20, with 665W maximum power output and efficiency measured at 21.4% making it ideal for the project at hand. Furthermore, with 600 panels the annual output of electricity is calculated at 614693 kWh, which covers 71% of the energy consumed at the Myloniana site.

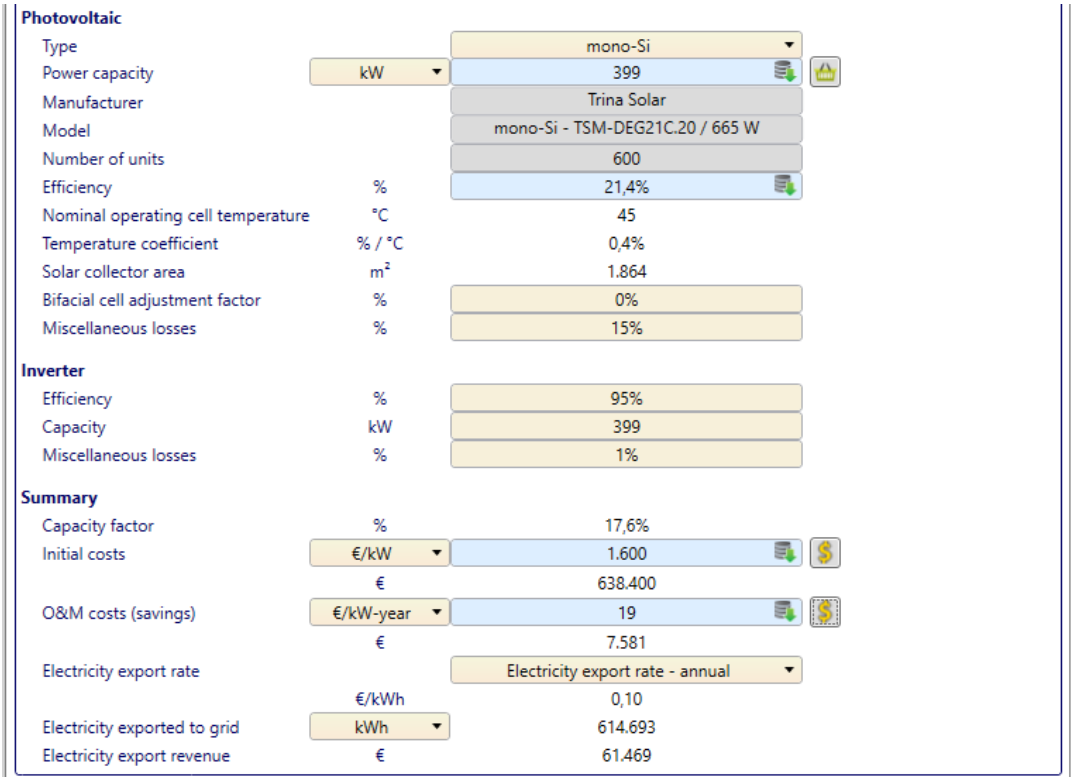

Photovoltaic		
Type		mono-Si
Power capacity	kW	399
Manufacturer		Trina Solar
Model		mono-Si - TSM-DEG21C.20 / 665 W
Number of units		600
Efficiency	%	21,4%
Nominal operating cell temperature	°C	45
Temperature coefficient	% / °C	0,4%
Solar collector area	m^2	1.864
Bifacial cell adjustment factor	%	0%
Miscellaneous losses	%	15%
Inverter		
Efficiency	%	95%
Capacity	kW	399
Miscellaneous losses	%	1%
Summary		
Capacity factor	%	17,6%
Initial costs	€/kW	1.600
	€	638.400
O&M costs (savings)	€/kW-year	19
	€	7.581
Electricity export rate		Electricity export rate - annual
	€/kWh	0,10
Electricity exported to grid	kWh	614.693
Electricity export revenue	€	61.469

Figure 18: *Panel characteristics*

Regarding the emission analysis of this proposal, also calculated with RETScreen expert software, the emissions of the existing network would be reduced significantly. Based on the data from DAPEEP AE regarding the energy mix by DEH, GHG emission factors for each fuel type by RETScreen and Greece's T&D (Transmission and Distribution) losses from World Bank, a gross annual GHG emission reduction of 227 tons of CO2 was calculated.

Base case electricity system (Baseline)

Fuel type	Fuel mix %	CO_2 emission factor kg/GJ	CH_4 emission factor kg/GJ	N_2O emission factor kg/GJ	Electricity generation efficiency %	T&D losses %	GHG emission factor $kgCO_2/kWh$
Natural gas	36,9%	49,6	0,0010	0,0009	45,0%	8,0%	0,433
Coal	15,0%	95,8	0,0150	0,0030	35,0%	8,0%	1,085
Wind	14,8%	0,0	0,0000	0,0000	100,0%	8,0%	0,000
Solar	12,9%	0,0	0,0000	0,0000	100,0%	8,0%	0,000
Hydro	8,7%	0,0	0,0000	0,0000	100,0%	8,0%	0,000
Oil (#6)	7,7%	77,8	0,0030	0,0020	30,0%	8,0%	1,023
Nuclear	2,7%	0,0	0,0000	0,0000	30,0%	8,0%	0,000
Biomass	1,2%	0,0	0,0320	0,0040	25,0%	8,0%	0,031
Geothermal	0,1%	0,0	0,0000	0,0000	30,0%	8,0%	0,000
Electricity mix	100,0%	110,5	0,0104	0,0030		8,0%	0,402

Baseline changes during project life

Figure 19: *Energy mix by DEH 2022*

The 92% reduction compared to electrical energy provided by the grid is equivalent to 97634 liters of gasoline not consumed, a very significant reduction. The proposed photovoltaic farm costs an estimated 638400€, without considering the possibility of a large battery system needed for the energy storage required for efficiency.

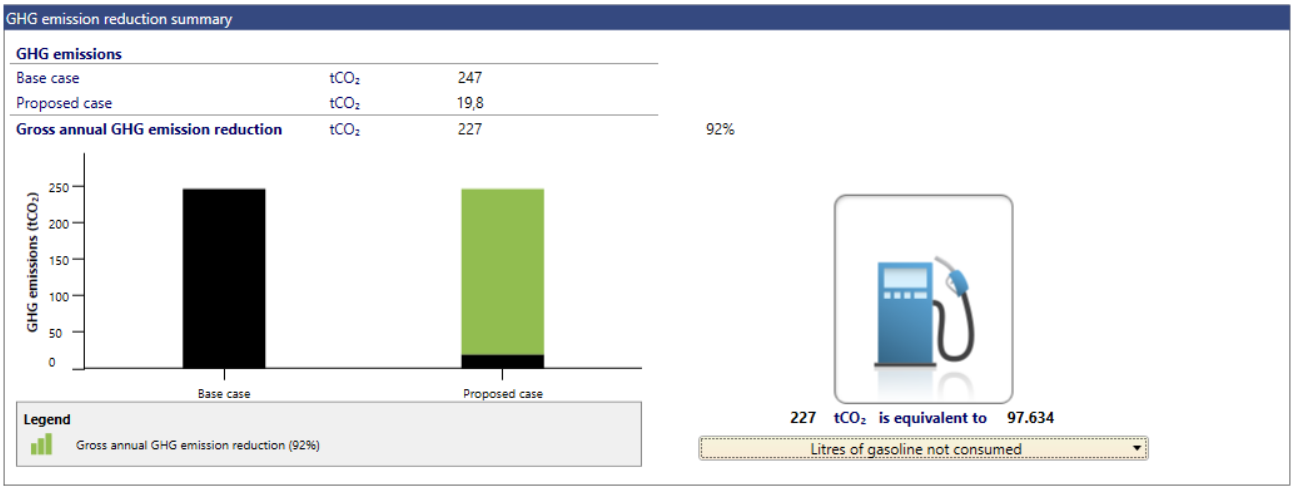

Figure 20: *GHG emission reduction*

2.5 Energy analysis using Global Solar Atlas

Global Solar Atlas (GSA), developed by the World Bank Group using data from Solargis, provides high-resolution solar resource data globally. It is primarily designed to support project developers and researchers.

Unlike RETScreen, which is a comprehensive analysis tool for calculating energy production, costs and emissions, GSA is mainly a data-rich mapping tool. It provides detailed solar irradiation (global horizontal irradiation, direct normal irradiation) and calculates the potential photovoltaic power output (PVOUT) for a given location and system configuration. Even though it does not perform financial analysis, it is essential for feasibility studies of renewable energy integration, allowing appraisal of the amount of electricity a PV system can produce.

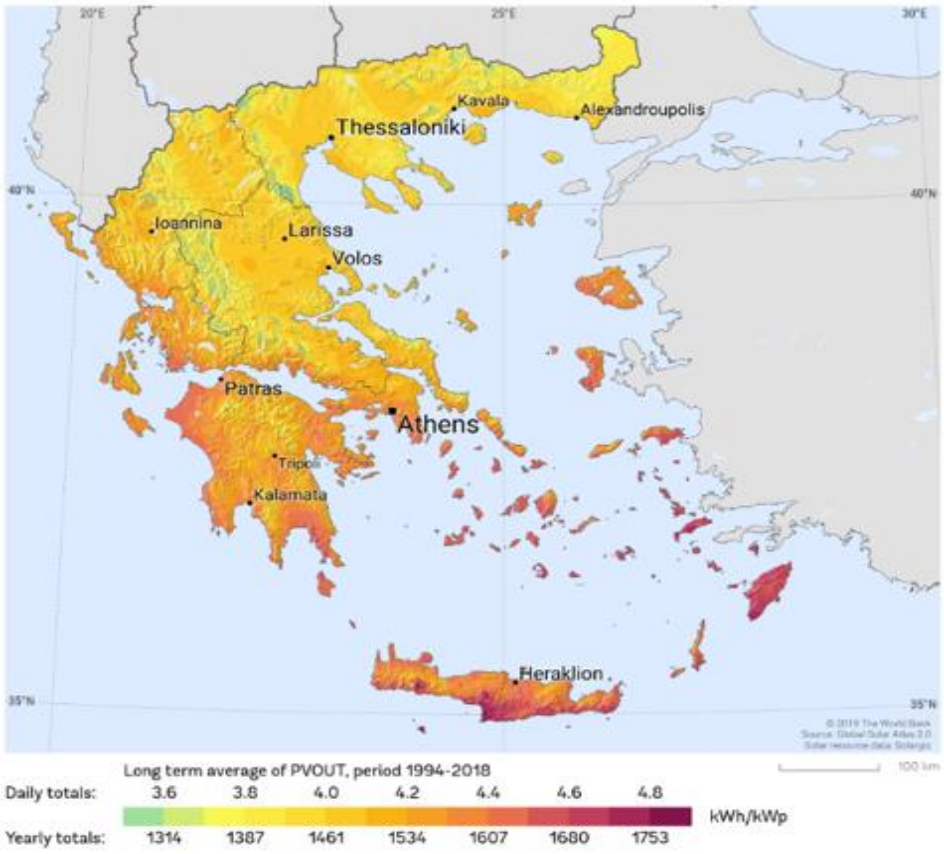

Figure 21: *PV power potential*

In this study, GSA was used to assess the solar potential for powering the Myloniana pumping stations. The annual demand of electricity, calculated to be 854483,864 kWh/year, was compared with the PV potential from GSA. The analysis used global horizontal irradiation (GHI) and direct normal irradiation (DNI) data for the region selected in Chania. A potential PV system was selected big enough to cover 71% of the pumping stations' electricity needs

The suggested installation has a capacity of 399 kWp, with a tilt of 27°, producing 617 MWh per year.

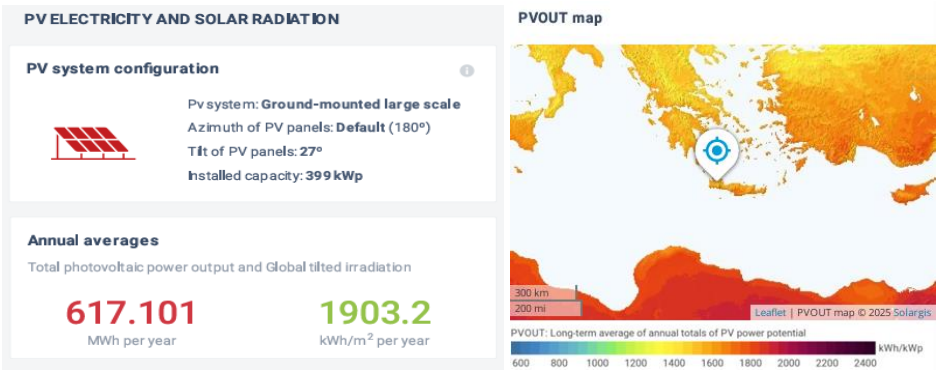

Figure 22: *PV system characteristics*

2.6 Leak detection simulations

A leak detection simulation was performed in the network using the Darwin Calibrator tool in WaterGEMS. This tool employs a genetic algorithm to identify potential leaks and their location. The emitter coefficient represents the flow rate through an opening at a given pressure, allowing the model to simulate the amount of water leaving a node as a function of its pressure.

The flow through an emitter is mathematically expressed as: $Q=kP^n$

where Q is the flow, k is the emitter coefficient (a property assigned to each node), P is the pressure, and n is the emitter exponent. The exponent n is globally defined in the calculation options of the run, and while dimensionless, it directly influences the units of k. By default, n=0.5, which corresponds to the typical behavior of flow through an orifice. This allows the hydraulic model to realistically represent leakage as a pressure-dependent outflow.

The input data required for the Darwin Calibrator included the hydraulic grade measurements at all the nodes and the flows in the pipes and pumps between reservoirs and tanks at the specific time being tested. The emitter coefficient was set between a minimum of 0 and a maximum of 0.5, where higher values indicate a higher probability of a leak at or near a node. Additionally, the maximum number of nodes that could exhibit leaks was defined as 100 [23], [24], [25], [26].

The 48-hour simulation model was used for this part of the study. It was extended to 72 hours to examine three consecutive days. The calibrations took place at specific times: day 1 at 3 AM (3 hours), day 2 at 4 AM (28 hours), day 3 at 5 AM (53 hours). This allowed the analysis to focus on the early morning, when water consumption is minimal. These hours are ideal as potential leaks are more likely to be detected during periods of low demand, avoiding false positives [27].

During the simulation, pipelines and pumps that were initially closed due to operational rules were kept inactive to prevent the algorithm from trying to optimize flows in these components.

Leak Detection at 3 hours

At 3 AM on day 1, the Darwin Calibrator identified 53 nodes with a probability of leakage. Among these, 8 nodes exhibited the maximum emitter coefficient of 0.5 L/min/(mH_2O)^n, indicating the highest risk of leak occurrence. The fitness score of this solution was 6, a great match between simulated and reference hydraulic conditions.

Figure 23: *Some potential leaks at 3 hours*

Leak detection at 28 hours

At 4 AM on day 2, 50 nodes were flagged as potential leaks. Thirteen of these reached the maximum emitter coefficient of 0.5 L/min/(mH_2O)^n, indicating higher risk. The fitness score in this calibration was 27, which is also a very close match.

Figure 24: *Some potential leaks at 28 hours*

Leak detection at 53 hours

At 5 AM on day 3, the detection identified 54 nodes with potential leaks, of which 17 nodes showed the highest emitter coefficient of 0.5 L/min/$(mH_2O)^{n.}$ These nodes should be closely monitored to prevent or mitigate leakage. The fitness score was calculated to 35.

Figure 25: *Some potential leaks at 53 hours*

The leak detection simulation using the Darwin Calibrator enabled identification of nodes with the highest potential for leakage over the three days examined. The analysis focused on early

morning to minimize interference from normal water consumption, providing a clearer assessment of potential losses. While the fitness scores indicate varying degrees of agreement between simulated and reference hydraulic conditions, the nodes with maximum emitter coefficient highlight areas that require monitoring and potential maintenance. These results demonstrate the utility of WaterGEMS' tool for proactive leak management and network optimization, even with simulated data.

Chapter 3: Results

3.1 Hydraulic performance

Hydraulic performance of the network was evaluated using both the 48-hour and annual simulations to assess system's ability to maintain sufficient pressures, adequate flows and acceptable tank levels under operational conditions. The analysis is focused on critical pipelines, tanks and junctions, as well as overall network performance.

Four representative tanks were selected to illustrate hydraulic grade over time. Graphs show the hourly variations, highlighting how the control rules worked and how their existence prevented critical shortages. The tanks chosen in the graphs are Tank AT, Tank Mournies, Tank Myloniana and Tank Freatiohremiasvl. Each one of them functions under different demand patterns and by different rules, which the graph validates.

Examining the graphs from the 48-hour simulation, tank AT shows a rapid increase in hydraulic grade until it stabilizes around 149 m. After this point the tank remains full for most of the simulation, with minor gradual decreases. This stability indicates that the rules successfully keep the tank at a specific level. Tank Mournies demonstrates a cyclical filling and emptying pattern throughout the 48 hours. The hydraulic grade varies from 106 m to 107 m with two distinct drops, followed by refills. Tank Myloniana exhibits the most pronounced variations among the four tanks analyzed. The sharp decreases before refilling are expected behavior for this tank due to the number of pumps and reservoirs close to it but also due to its rules (provides water to a big part of the network). Tank Freatiohremiasvl exhibits a highly repetitive and frequent pattern. The hydraulic grade fluctuates between 81 m and 86 m. This rapid discharge and refill show how the tank operates as a pressure-regulating buffer. It absorbs the upstream high pressure and helps reduce it. The plateau between 30-36 hours suggests a temporary equilibrium, likely due to steady network conditions.

48-hour simulation:

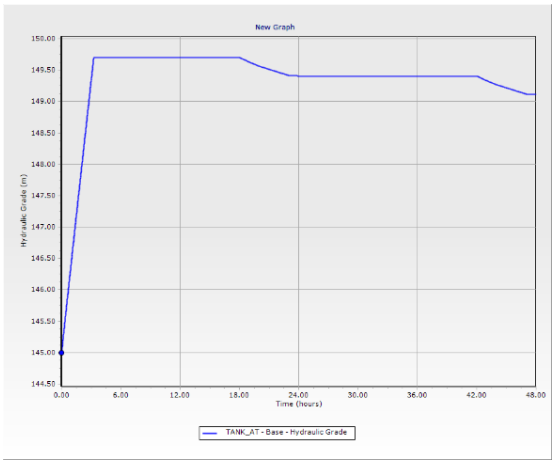

Graph 4: *Tank AT*

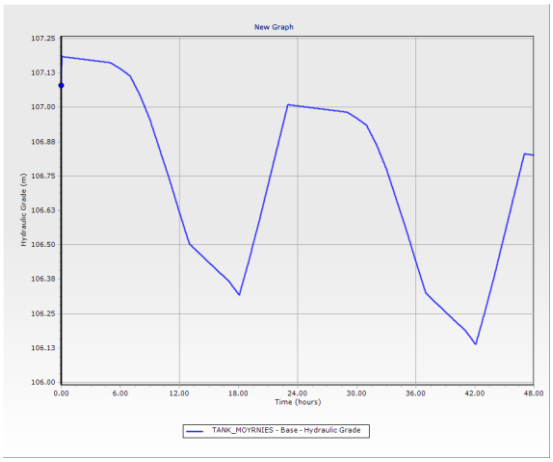

Graph 5: *Tank Mournies*

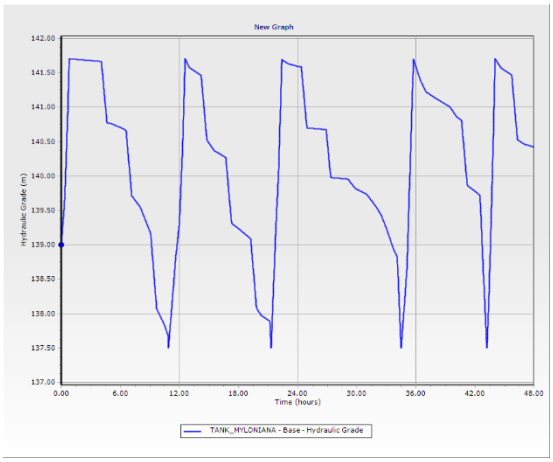

Graph 6: *Tank Myloniana*

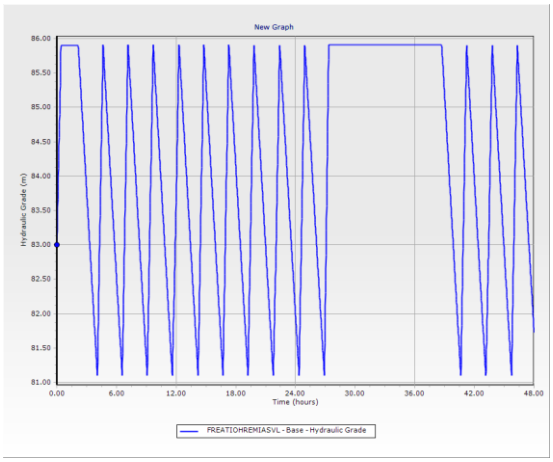

Graph 7: *Tank Freatiohremiasvl*

Examining the graphs from the annual simulation, tank AT seems to have a consistent pattern of operation. The hydraulic grade ranges between 145 and 150 m, which is an indicator of the proper function of the rules. In tank Mournies, more irregular shifts in hydraulic grade are observed and prolonged periods of stability. When demand increases, rapid drops are detected. The seasonal rule is definitely in effect, which is very clear in the graph through the peak demand months. In tank Myloniana, the hydraulic grades ranges between 136 and 142 m. There is understandably high damnd, which is met also by using the pumping stations nearby. Also, the importance of reservoirs near this tank is highlighted. The annual results for Tank Freatiohremiasvl show somewhat stability in hydraulic grade. The operation is consistent with its primary role; to reduce pressure. The tank does not experience extreme drops, which confirms its effectiveness throughout the year.

Annual simulation:

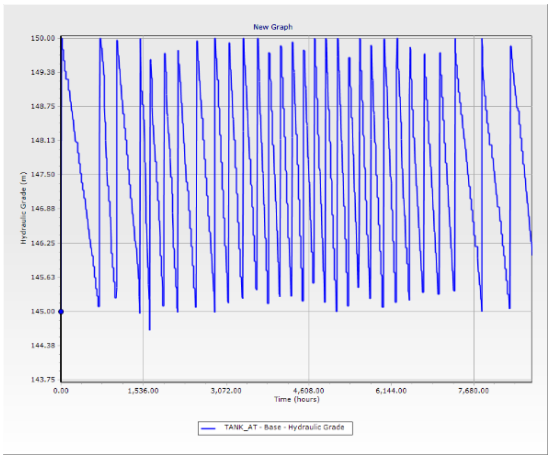

Graph 8: *Tank AT*

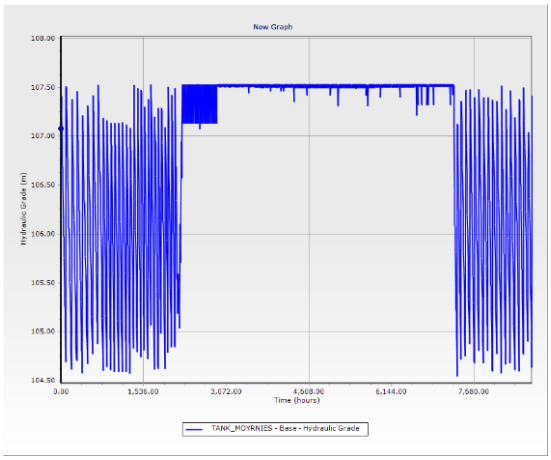

Graph 9: *Tank Mournies*

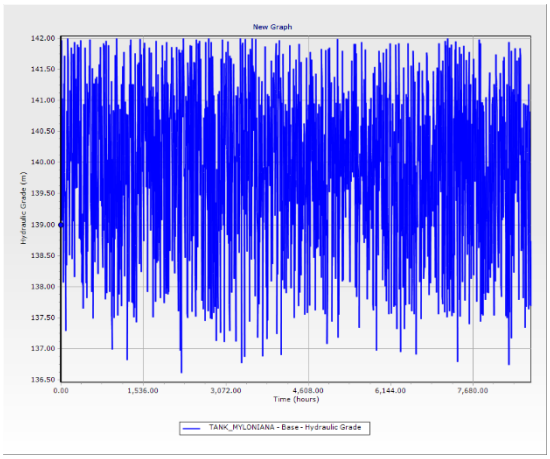

Graph 10: *Tank Myloniana*

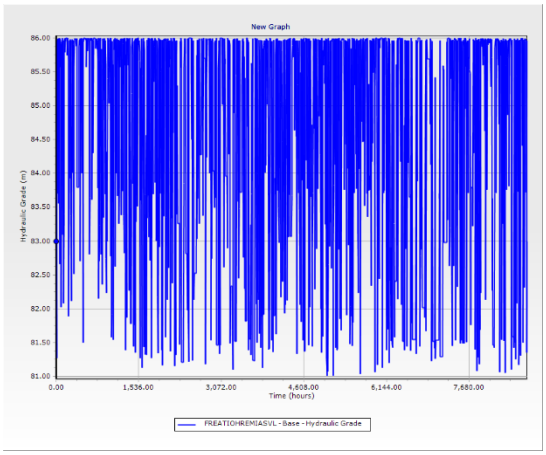

Graph 11: *Tank Freatiohremiasvl*

Two main pipes were selected for examination of their flow behavior. Graphs show flow variations in response to demand fluctuations and to the control rules. In the 48-hour simulation, flow follows the demand patterns for every hour, confirming the correct implementation of the control rules. The flow in the graphs aligns with the demand patterns created. Peaks correspond to higher consumption, such as morning and evening hours, and valleys correspond to lower demand, probably after midnight. Correctly implemented the control rules, the system adjusts the flow distribution to agree with real-time needs.The rapid transitions are due to the activation and deactivation of the pumps.

48-hour simulation:

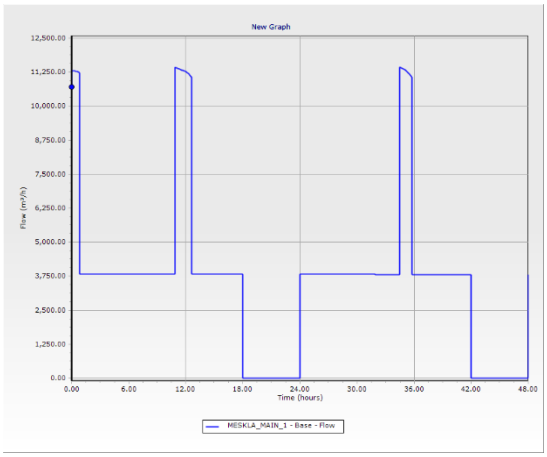

Graph 12: *Pipe MESKLA_MAIN_1*

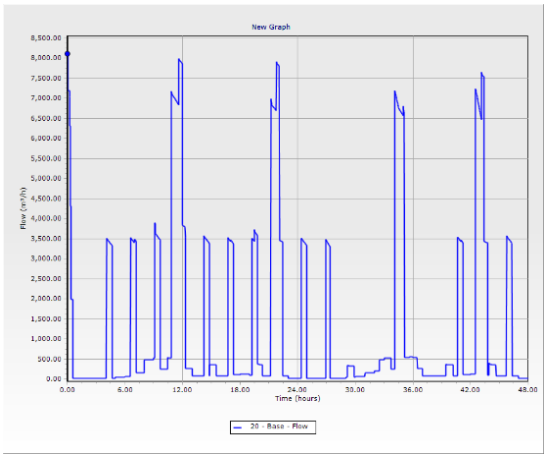

Graph 13: *Pipe 20*

In the annual simulation, it is very clear how pipe MESKLA_MAIN_1 closes seasonally and flow is redirected through alternative means and pumping stations to the network. This pattern reflects on the complexity of the network, ensuring water flow during the dry season. Graphs also indicate the distribution through the year is smooth, well-coordinated, while maintaining stability. The ability of the network to adapt to both hourly and seasonal needs demonstrates efficiency.

Annual simulation:

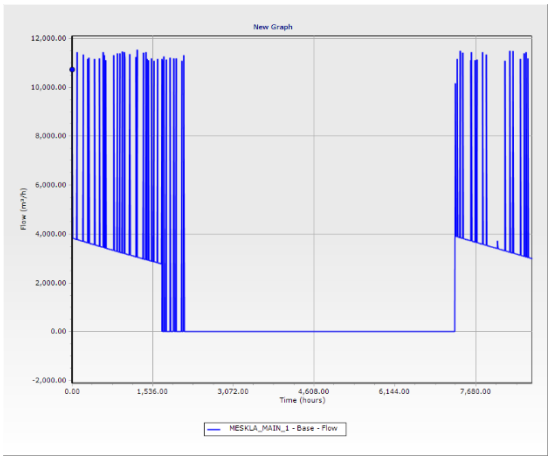

Graph 14: *Pipe MESKLA_MAIN_1*

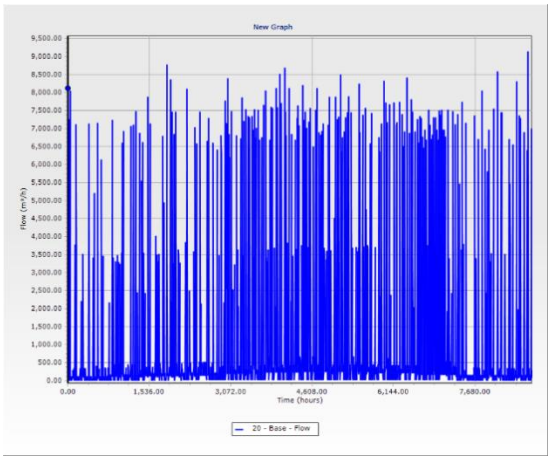

Graph 15: *Pipe 20*

Two randomly selected junctions with varying demands were selected to demonstrate local hydraulic performance. Both simulations confirmed that minimum pressure requirements were met, even during peak demand or seasonal source reduction.

In the 48-hour simulation, the junctions reflect the way demand rises during the morning and the way it falls during the nighttime. The graphs show that pressure levels are maintained above the minimum required thresholds. The efficient correspondence between demand patterns and pressure stability indicates the system is operating properly.

48-hour simulation:

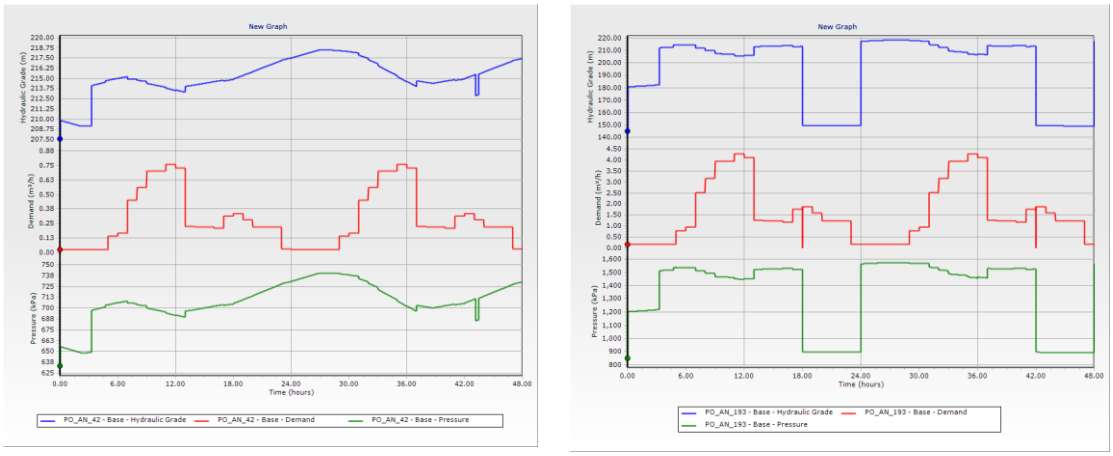

Graph 16: *Junctions PO_AN_42 and PO_AN_193*

The annual simulation provides a broader perspective on demand and supply conditions through seasonal variations. The graphs highlight that even during periods of reduced availability, the junctions continue to receive adequate pressure.

Annual simulation:

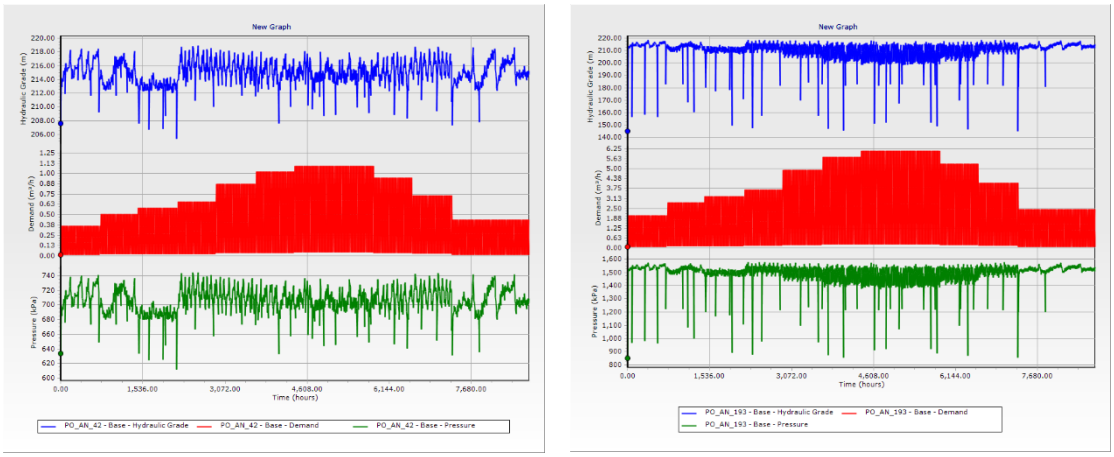

Graph 17: *Junctions PO_AN_42 and PO_AN_193*

The final graphs present the total water demanded, supplied and stored across the entire network during each simulation. This visualization highlights the effectiveness of the rules for all systems' components, showing how balanced supply and demand are both short- and long-term.

The blue line shows the expected daily fluctuations. The red follows the demand curve and demonstrates the rules' application in order to match supply with consumption. The green line reflects the dynamics of the tanks: during low-demand periods, storage increases as surplus supply fills reservoirs and during high-demand periods, stored water is released to supplement the direct supply. This pattern highlights the system's stability and its ability to prevent shortages.

48-hour simulation:

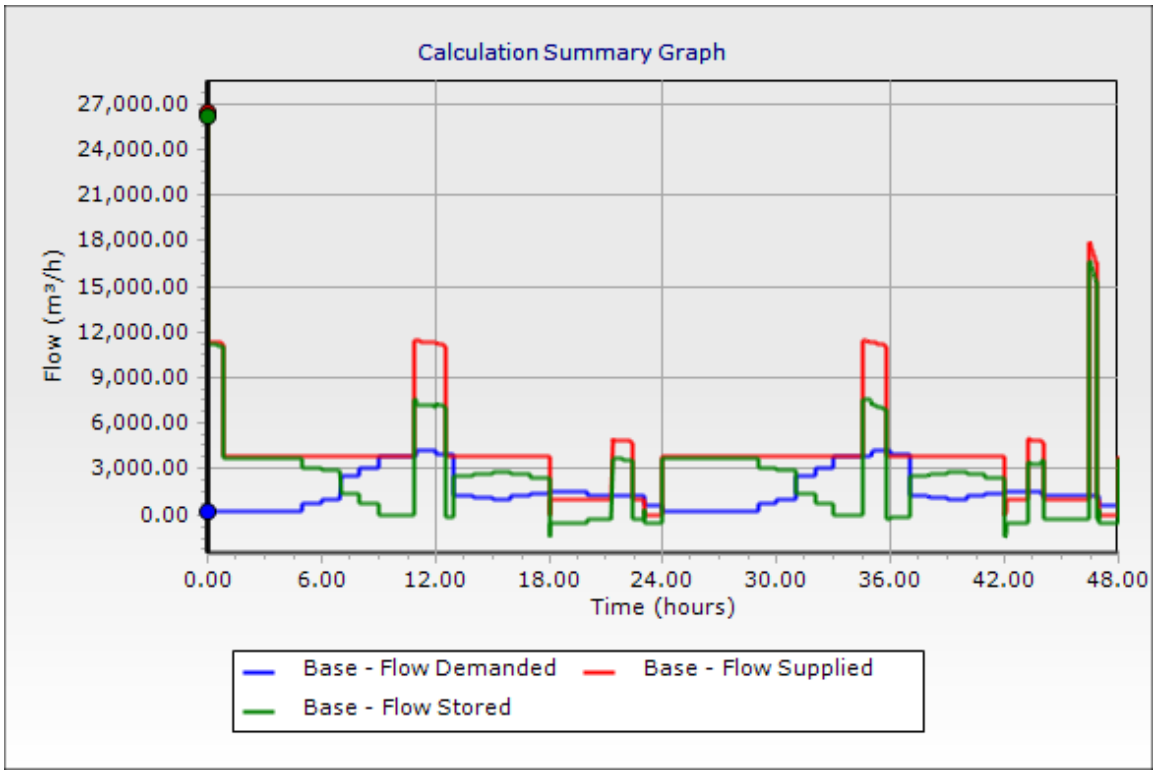

Graph 18: *System's flow*

Over the course of the year, the patterns become more complex due to seasonal variations in demand and operation adjustments. The blue line shows a gradual rise, particularly during summer. The red supply line responds to the visible high demand by intensifying pump activity. The green storage line has frequent positive and negative swings, reflecting the continuous use of reservoirs to buffer seasonal extremes. The supply and demand are in close alignment.

Annual simulation:

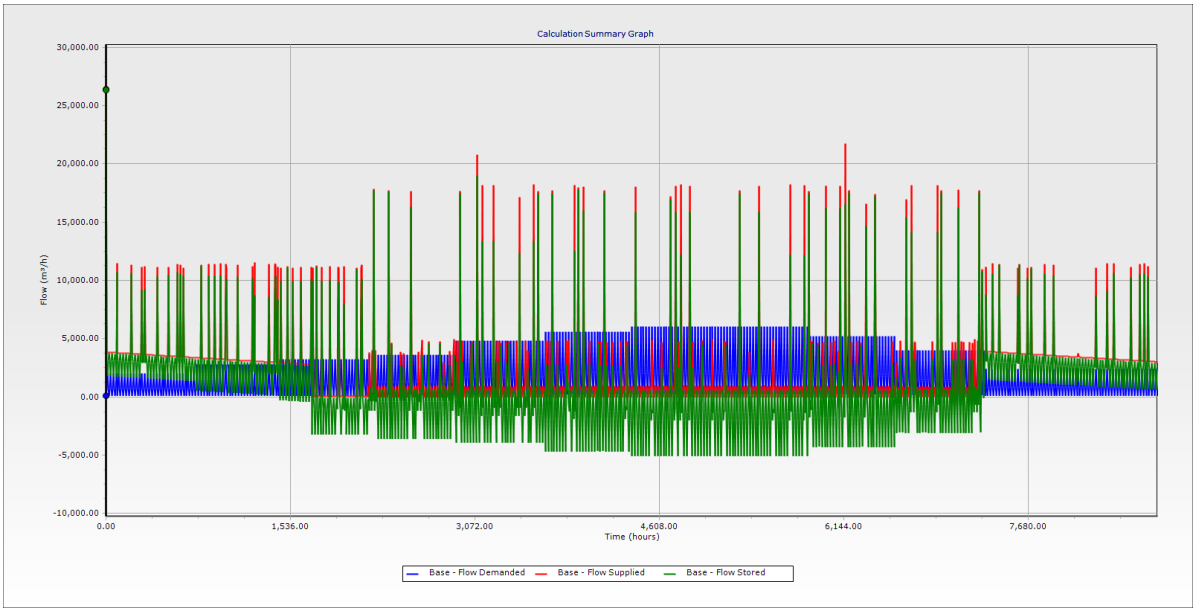

Graph 19: *System's annual flow*

3.2 Pump operation

Pump operation was evaluated in both simulations, with the objective of assessing how the defined control rules managed pump activity. The analysis focused on specific pumps, which had a critical role in transferring water between reservoirs and tanks.

In the 48-hour simulation, pump behavior closely followed the hourly demand patterns. Pumps were activated primarily to help refill tanks once their water levels dropped near the minimum thresholds. Pump activation and deactivation patterns reflected demand variations, showing that the control rules successfully prevented service interruptions.

In the annual simulation, pump operation displayed a more complex pattern due to the seasonal variations in demand and the closure of MESKLA_MAIN_1 pipeline during the dry season. During those months, certain pumps were required to operate more intensively, as flow was redirected. The results highlight how the rules prioritized refilling tanks under high-demand conditions while reducing pump activity during periods of lower consumption.

The analysis confirmed that the control rules effectively balanced the need for water supply with the minimization of unnecessary pump cycling. This ensured operational stability while reducing wear on the pumps.

3.3 Comparison of scenarios

The comparison between the two simulations highlights both the short-term responsiveness of the system and its long-term adaptability. While the 48-hour model was used to validate the control rules and evaluate the operational dynamics, the annual model provided insights into how these rules function under higher demand and complex conditions.

When examining tanks, the shorter simulation showed stable daily cycles with refilling and emptying occurring in specific patterns that aligned with morning and evening demand peaks. In contrast, the longer simulation demonstrated how tank behavior is influenced by seasonal changes in demand and the closure of the main pipeline.

In terms of pipe flows, the 48-hour case reflected immediate demand-driven fluctuations and confirmed the functionality of the rules. The annual case highlighted the importance of the seasonal rule with the most important graph being the MESKLA_MAIN_1. In the graph, it was clear the flow redirection in summer months was for continuous supply all year.

The junctions followed their assigned patterns (daily and daily 1). Pressure and demand matched daily consumption cycles, with pressure remaining above minimum. In the annual simulation, it was confirmed that the system created can sustain these levels of pressure and demand during periods of higher consumption or reduced natural inflows.

Finally, for the overall supply-demand balance, the 48-hour simulation highlighted the ability of the rules to meet hourly consumption while maintaining stable storage. In the annual simulation, this balance was maintained as well, but the graphs revealed more pronounced swings in storage during summer. These fluctuations reflect the use of reservoirs as buffers during high-demand months and demonstrate the adaptability of the system to both daily and seasonal conditions.

Overall, the effectiveness of the control rules was validated under normal operating conditions. The systems' capacity to manage seasonal stress in more demanding operating scenarios was also validated. Together, the two simulations confirmed the operating reliability of the system and underlined the importance of pumping and storage during the dry period.

3.4 Feasibility analysis of renewable integration

The integration of renewable energy sources, particularly PV systems, was assessed for environmental and economic feasibility using RETScreen and Global Solar Atlas. Simulation results demonstrated that a properly sized PV installation could cover a significant portion of the electricity demand associated with pump operation could be covered by a properly sized PV installation. There are two options to minimize energy losses from PV: net metering and batteries.

By incorporating net metering in the network, excess energy generated by on-site photovoltaic systems is fed into the grid and offset against consumption to reduce operational electricity costs. This method could be very effective for the case analyzed before, the Myloniana pumping stations, since they require electricity during periods of lower or no solar production.

Also, batteries are an option for storing surplus energy generated at midday from PV systems. Then, this energy can be used when necessary, even at night, while reducing reliance on grid electricity. Furthermore, battery storage can provide protection and security against grid outages, ensuring stable operation.

Both solutions, though, are not feasible for the water supply network in Chania. Net metering is not applicable, since it is unavailable in this area and batteries involve very high costs. As a result, the previously proposed scenario of 615000 kWh would be inefficient due to the loss of the largest part of the energy produced. At this point, a better solution would be to construct a smaller plant of PV for Myloniana pumping stations [28].

The operating hours of the pumps during sunlight hours, specifically during the period of 9 AM to 4 PM, added up to 645 hours. So, the annual consumption of electricity at these hours was calculated to be 204127 kWh (roughly 23% of the total annual energy consumption). Therefore, a smaller-scale plant would be a better choice to cover this daytime demand.

Average hourly profiles

Direct normal irradiation [Wh/m²]

	Jan	Feb	Mar	Apr	May	Jun	Jul	Aug	Sep	Oct	Nov	Dec
0 - 1												
1 - 2												
2 - 3												
3 - 4												
4 - 5												
5 - 6												
6 - 7												
7 - 8					196	341	268	84				
8 - 9				281	384	508	514	457	191			
9 - 10			253	387	490	615	632	586	467	191		
10 - 11		177	404	468	568	698	719	676	546	431	187	
11 - 12	259	381	451	523	622	751	777	737	608	474	396	246
12 - 13	356	403	471	546	646	775	806	764	627	485	406	323
13 - 14	353	396	472	552	645	778	812	769	626	484	411	318
14 - 15	338	381	469	539	631	772	805	759	605	468	384	300
15 - 16	324	353	445	509	603	738	783	730	569	436	339	275
16 - 17	271	311	396	455	552	684	730	681	510	362	279	226
17 - 18	110	257	331	384	479	614	652	600	424	245	55	
18 - 19		48	188	279	379	508	544	470	217			
19 - 20				41	142	301	327	138				
20 - 21						16	18					
21 - 22												
22 - 23												
23 - 24												
Sum	2,010	2,707	3,879	4,964	6,336	8,100	8,388	7,450	5,391	3,574	2,458	1,688

Figure 26: *Solar irradiation per month and hour*

A quick analysis on RETScreen or GSA shows that a 167 kW plant with 250 PV panels would generate sufficient power for operating hours in the Myloniana pumping stations during sunlight hours. This smaller power plant has the same technical characteristics as the larger system but costs only 266000€ (roughly one-third of the previous estimated cost).

This solution offers several advantages. It is cost-effective, easier to construct and maintain and reduces the reliance on grid electricity, thereby lowering GHG emissions. This smaller power plant covers approximately 23% of the annual pumping station demand in electricity.

Chapter 4: Conclusions and proposed solutions

4.1 Summary of key findings

The study demonstrated the importance of sustainable water networks in addressing urbanization, climate change and rising demand. Smart water networks, with their automated controls and real-time monitoring, were shown to improve efficiency, decision-making and long-term resilience. With over 111,000 population and significant seasonal fluctuations brought on by tourism and agriculture, the water delivery network of Chania was chosen as the case study. To depict the region's wet and dry environment, accurate hydraulic modeling was crucial.

The network was modeled using WaterCAD and WaterGEMS software. Both programs were introduced, highlighting their features, with WaterGEMS offering extended capabilities.

The Meskla springs, the Valsamiotis dam, and the crucial significance of certain pumping stations were highlighted in the detailed description of the network under study. These elements make ensuring that water is distributed among several municipalities in response to different seasonal demands.

Two main simulations were developed:

- A 48-hour simulation, designed as a baseline for validating rules and overall hydraulic consistency. Demand-based, tank-level and time-based control rules were applied to replicate operational strategies, ensuring a continuous supply during short-term fluctuations.
- An annual simulation, which incorporated seasonal variations, tourism-driven demand surges and agricultural water usage. A key seasonal rule was introduced to simulate the closure of theMESKLA_MAIN_1 pipeline during the dry season, forcing greater reliance on pumping stations.

An energy analysis was conducted using RETScreen Expert and Global Solar Atlas. The Myloniana pumping stations was selected as a case study due to its high energy demand. RETScreen showed that installing a 399 kWp photovoltaic system could cover 71% of the station’s annual electricity needs., while reducing CO_2 emissions by 227 tons per year. GSA confirmed the strong polar potential in the area, validating the feasibility of large-scale

renewable integration. The minimal difference (0.37% deviation) between RETScreen and GSA confirms the reliability of the energy simulation results, providing confidence in the proposed PV integration strategy.

However, the lack of net metering and the high cost of batteries limit the viability of the large-scale PV system. For the Myloniana pumping stations, a smaller 167 kWp PV plant was suggested instead, which could supply 23% of its yearly electricity needs during the day. This option balances cost, technical feasibility and environmental benefits, reducing both grid dependence and GHG emissions.

Leak detection using the Darwin Calibrator tool, was performed. The 48-hour simulation was extended to 72 hours to identify multiple nodes with a high probability of leakage, particularly during low-demand hours. Approximately 50 nodes in each scenario were detected, which underlines the potential to support proactive leak management and improve network efficiency.

Hydraulic performance showed that tanks, pipes and junctions operated reliably under short- and long-term conditions. The 48-hour model showed clear daily cycles, while the annual simulation revealed the impact of seasonal demand and the closure of MESKLA_MAIN_1. Supply, demand and storage remained balanced with reservoirs buffering fluctuations.

Pump operation followed demand patterns in both simulations. Pumps refilled tanks efficiently and worked harder during the annual model to reroute flow in summer.

Finally, a direct comparison of scenarios demonstrated how the 48-hour simulation validated the rules and daily operation, while the annual proved the system's resilience under stress conditions. The significance of pumping and storage capacity was emphasized by seasonal fluctuations.

Overall, the findings confirm that the network operates reliably under both short-term and long-term conditions. Control rules, combined with adequate storage and pumping capacity, ensure resilience against daily and seasonal fluctuations. At the same time, renewable energy integration presents an opportunity for greater sustainability, provided that investments are tailored to local feasibility.

4.2 Proposed solutions and implementation strategies

The results underline the need for a structured strategy that addresses hydraulic performance, energy efficiency and long-term sustainability. The water supply network in Chania can be made resilient to changes and different demand pressures by combining operational enhancements, technology advancements, and the integration of renewable energy sources.

Operational control rules should continue to be monitored and refined, particularly in response to seasonal variations in demand and source availability. Periodic recalibration of pumps, tanks and critical junctions is essential to guarantee consistent hydraulic performance. Adaptive management as circumstances change will be ensured by routinely reevaluating system performance using updated population and demand data.

According to the feasibility analysis, a large-scale PV installation is not viable under current regulatory and financial conditions. Instead, a smaller PV plant at the Myloniana pumping stations is recommended. This system can lower the overall carbon footprint, lessen reliance on the grid, and meet demand during the day. To increase the system's financial advantages, net metering ought to be explored in the future if at all feasible. Additionally, as technology costs change, chances to incorporate additional renewable energy sources should be investigated.

Gradual integration of smart water network features will improve operational efficiency. This includes automated alerts for anomalous occurrences, SCADA system integration, and real-time flow and pressure monitoring. Such tools will make it possible to respond to anomalies more quickly, increase operational transparency, and make better-informed decisions.

The Darwin Calibrator tool's identification of nodes with a high likelihood of leakage emphasizes the significance of a preventative leak detection and repair program. Nodes with the highest emitter coefficients should be prioritized to ensure targeted interventions where efficiency gains are maximized. This approach can significantly reduce non-revenue water while improving the reliability of supply.

To optimize energy use, pump schedules should be reviewed with a view to minimizing unnecessary cycling and adapting to high-demand periods. Finally, using variable-speed drives and energy-efficient pumps could further increase operational stability and lower electricity costs.

Bibliography

[1] “Sustainable and resilient water infrastructures and distribution networks | EESC.” Accessed: Sep. 23, 2025. [Online]. Available: https://www.eesc.europa.eu/en/news-media/press-summaries/sustainable-and-resilient-water-infrastructures-and-distribution-networks

[2] Ε. Καραθανάση, Δ. Πάτρας Δημήτριος Βακόνδιος, Δ. Σύρου Χρήστος Μπίμης, Δ. Λιβαδειάς Δέσποινα Μπώκου, and Δ. Λέσβου Ελευθέριος Σφυρής, “ΥΠΟΛΟΓΙΣΜΟΣ ΥΔΑΤΙΚΟΥ ΙΣΟΖΥΓΙΟΥ ΚΑΙ ΔΕΙΚΤΩΝ ΑΠΟΔΟΣΗΣ Ομάδα Εργασίας”.

[3] “IWA Water Balance | LEAKSSuite Library.” Accessed: Sep. 23, 2025. [Online]. Available: https://www.leakssuitelibrary.com/iwa-water-balance/

[4] “Smart Water Networks: The Future of Utility Optimization.” Accessed: Sep. 23, 2025. [Online]. Available: https://waltero.com/resources/smart-water-networks/

[5] B. Z. Rousso, M. Lambert, and J. Gong, “Smart water networks: A systematic review of applications using high-frequency pressure and acoustic sensors in real water distribution systems,” *J Clean Prod*, vol. 410, p. 137193, Jul. 2023, doi: 10.1016/J.JCLEPRO.2023.137193.

[6] “The Essential Guide to Smart Water Networks | Wint.” Accessed: Sep. 23, 2025. [Online]. Available: https://wint.ai/blog/the-essential-guide-to-smart-water-networks/

[7] “The Smart Water Journey - SWAN Forum.” Accessed: Sep. 23, 2025. [Online]. Available: https://swan-forum.com/smart-water-network/

[8] P. M. Soupios, M. Kouli, F. Vallianatos, A. Vafidis, and G. Stavroulakis, “Estimation of aquifer hydraulic parameters from surficial geophysical methods: A case study of Keritis Basin in Chania (Crete - Greece),” *J Hydrol (Amst)*, vol. 338, no. 1–2, pp. 122–131, May 2007, doi: 10.1016/j.jhydrol.2007.02.028.

[9] “Chaniá Climate, Weather By Month, Average Temperature (Greece) - Weather Spark.” Accessed: Sep. 23, 2025. [Online]. Available: https://weatherspark.com/y/90522/Average-Weather-in-Chani%C3%A1-Greece-Year-Round#Sections-Rain

[10] K. P. Tsagarakis, G. E. Dialynas, and A. N. Angelakis, “Water resources management in Crete (Greece) including water recycling and reuse and proposed quality criteria,” *Agric Water Manag*, vol. 66, no. 1, pp. 35–47, Apr. 2004, doi: 10.1016/J.AGWAT.2003.09.004.

[11] “(PDF) GIS - based water management in the Chania area, Western Crete.” Accessed: Sep. 23, 2025. [Online]. Available: https://www.researchgate.net/publication/237539725_GIS_-_based_water_management_in_the_Chania_area_Western_Crete

[12] “Φράγμα Βαλσαμιώτη – ΟΑΚΑΕ.” Accessed: Sep. 23, 2025. [Online]. Available: https://oakae.gr/portfolio-item/fragma-valsamioti/

[13] “Φράγμα Βαλσαμιώτη - Βικιπαίδεια.” Accessed: Sep. 23, 2025. [Online]. Available: https://el.wikipedia.org/wiki/%CE%A6%CF%81%CE%AC%CE%B3%CE%BC%CE%B1_%CE%92%CE%B1%CE%BB%CF%83%CE%B1%CE%BC%CE%B9%CF%8E%CF%84%CE%B7

[14] Μ. ΘΕΟΔΩΡΑΚΗ, “ΜΕΛΕΤΗ ΦΡΑΓΜΑΤΟΣ ΒΑΛΣΑΜΙΩΤΗ ΝΟΜΟΥ ΧΑΝΙΩΝ,” *Νέα Κρήτη*, Feb. 2019, Accessed: Sep. 23, 2025. [Online]. Available: https://apothesis.lib.teicrete.gr/bitstream/handle/11713/2600/2009theodoraki.pdf?sequence=1&isAllowed=y

[15] “Lake Agia - Wikipedia.” Accessed: Sep. 23, 2025. [Online]. Available: https://en.wikipedia.org/wiki/Lake_Agia

[16] “Deyach Water And Wastewater Laboratory - Δ.Ε.Υ.Α. ΧΑΝΙΩΝ.” Accessed: Sep. 23, 2025. [Online]. Available: https://deyach.gr/deyach-water-and-wastewater-laboratory/

[17] D. J. Mehta, V. Yadav, S. I. Waikhom, and K. Prajapati, “DESIGN OF OPTIMAL WATER DISTRIBUTION SYSTEMS USING WATERGEMS: A CASE STUDY OF SURAT CITY.”

[18] D. Charchousi *et al.*, “AN ASSESSMENT APPROACH TO INVESTIGATE CLIMATE CHANGE IMPACTS IN CHANIA GROUNDWATER SYSTEM,” 2018. [Online]. Available: https://www.researchgate.net/publication/327972245

[19] B. Brahmamiah, K. Surendra, and P. Vani, “A comprehensive analysis of the water distribution network by using waterGEMS software,” in *IOP Conference Series: Earth and Environmental Science*, Institute of Physics, 2024. doi: 10.1088/1755-1315/1409/1/012005.

[20] S. S. Pathan and U. J. Kahalekar, “Design of Optimal Water Supply Network and Its Water Quality Analysis by using WaterGEMS,” NCKITE, 2013.

[21] C. S. Psomopoulos, G. C. Ioannidis, S. D. Kaminaris, K. D. Mardikis, and N. G. Katsikas, “A Comparative Evaluation of Photovoltaic Electricity Production Assessment Software (PVGIS, PVWatts and RETScreen),” in *Environmental Processes*, Springer Basel, Nov. 2015, pp. S175–S189. doi: 10.1007/s40710-015-0092-4.

[22] D. Thevenard, G. Leng, and S. Martel, “THE RETSCREEN MODEL FOR ASSESSING POTENTIAL PV PROJECTS.”

[23] “OpenFlows | Water Infrastructure - Performing Leakage Detection Using Darwin Calibrator - Communities.” Accessed: Sep. 23, 2025. [Online]. Available: https://bentleysystems.service-now.com/community?id=kb_article&sysparm_article=KB0057938

[24] “OpenFlows | Water Infrastructure - Performing Leakage Detection Using Darwin Calibrator - Communities.” Accessed: Sep. 23, 2025. [Online]. Available: https://bentleysystems.service-now.com/community?id=kb_article_view&sysparm_article=KB0057938

[25] “OpenFlows | Water Infrastructure - Water Model Calibration Tips - Communities.” Accessed: Sep. 23, 2025. [Online]. Available: https://bentleysystems.service-now.com/community?id=kb_article_view&sysparm_article=KB0016100

[26] “OpenFlows | Water Infrastructure - Using Darwin Calibrator - Communities.” Accessed: Sep. 23, 2025. [Online]. Available: https://bentleysystems.service-now.com/community?id=kb_article_view&sysparm_article=KB0015551

[27] “Εντοπισμός διαρροών και προτάσεις μείωσης του Μη Ανταποδοτικού Νερού στο δίκτυο ύδρευσης της Παλιάς Πόλης του Ηρακλείου”, doi: 10.26233/HEALLINK.TUC.103850.

[28] “Τι είναι ο ταυτοχρονισμένος ενεργειακός συμψηφισμός 2025 | Solarway.” Accessed: Sep. 23, 2025. [Online]. Available: https://solarway.gr/taftoxronismenos-energeiakos-sympsifismos/